Vietnam Journal of Earth Sciences, 44(3), 343-368, https://doi.org/10.15625/2615-9783/17002

Vietnam Academy of Science and Technology
Vietnam Journal of Earth Sciences
http://www.vjs.ac.vn/index.php/jse

Petrology of the Permian-Triassic granitoids in Northwest Vietnam and their relation to the amalgamation of the Indochina and Sino-Vietnam composite terranes

Tuan-Anh Tran[1], Hoa Tran-Trong[1], Can Pham-Ngoc[*1], J. Gregory Shellnutt[2], Thuy Thi Pham[3], Andrey E. Izokh[4], Phuong-Lien T. Pham[1], Somsanith Duangpaseuth[5], Oneta Soulintone[5]

[1]*Institute of Geological Sciences, VAST, Hanoi, Vietnam*
[2]*Department of Earth Sciences, National Taiwan Normal University, Taipei 11677, Taiwan*
[3]*Department of Geosciences, National Taiwan University, Taipei 106, Taiwan*
[4]*Institute of Geology and Mineralogy, Siberian Branch of Russian Academy of Sciences, Novosibirsk, Russia*
[5]*Cabinet of Science and Technology of Laos, Vientiane, Laos*

Received 19 May 2021; Received in revised form 28 December 2021; Accepted 02 March 2022

ABSTRACT

Granitoids from seven massifs in northwest Vietnam, including I-type granites (Nam Meng, Nam Rom, and Song Ma massifs) and S-type granites (Pu Si Lung, Kim Boi, Muong Lat, and Sam Son massifs) that distributed along the Dien Bien-Song Ma fault at the northern part of Truong Son Fold Belt, were studied to understand the mineralogy, geochemistry, Nd-Sr isotopes, and U-Pb zircon geochronology. The I-type granitoid rocks vary from gabbro diorite to diorite and granodiorite to granite (SiO_2 = 52.4-71.1 wt.%) and from calc-alkaline to high K calc-alkaline to shoshonite (Nam Rom massif) series. Biotite in the I-type granitoid rocks has high Mg, intermediate to high Ti, and low Al. The ASI varies from 0.64 to 1.14 (metaluminous); K/Na = 0.1-0.7; ratios of K/Rb, Rb/Sr and Rb/Ba varies from 179-334, 0.40-3.50, and 0.16-0.38; $[La/Sm]_N$, $[La/Yb]_N$ and $[Gd/Yb]_N$ are varies within 1.08-4.92, 1.57-27.3, and 1.07-3.72, respectively. Their $^{87}Sr/^{86}Sr$ and ƐNd(t) are highly enriched, respectively, from 0.7072 to 0.7319 and -12.2 to -6.67. The I-type granitoid rocks may be mixtures between mantle-derived and crustal components based on geochemical characteristics. In contrast, the Nam Meng magma was mantle-dominated, and the Nam Rom and Song Ma magmas were crustal-dominated. The S-type granitoid rocks include biotite granite and two-mica granite (SiO2 = 68.9-73.0 wt.%), varying from high K calc-alkaline to shoshonite series. The S-type granitoid rocks are distinct from the I-type granitoid rocks by sillimanite, cordierite, and muscovite. Biotite in the S-type granitoid rocks has high Ti and Al and low Mg. The mineral was partially replaced by muscovite. The ASI varies from 1.1 to 1.85 (peraluminous); K/Rb, Rb/Sr, and Rb/Ba vary within 161-188, 0.37-3.50, and 0.15-0.98; [La/Sm]N, [La/Yb]N and [Gd/Yb]N vary within 2.28-3.90, 5.93-16.8, and 1.72-2.93, respectively. The S-type granitoid rocks also have high $^{87}Sr/^{86}Sr$(i) (0.7227-0.7335) and low ƐNd(t) (-12.4 to -9.8) with TDM = 2.11-2.71 B.y., indicating a mature crust protolith. The in situ zircon U-Pb ages of the I-type granites are 289-296 Ma (Nam Meng massif) and 245-225 Ma (Nam Rom and Song Ma massifs), while those of the S-type granitoid rocks (Kim Boi and Muong Lat massifs) are 242-235 Ma. The above data suggest that the Indochina and Sino-Vietnam composite terranes produced the Permian-Triassic granitoid rocks in northwest Vietnam. The convergence had led to subduction activity forming Nam Meng granitoid, syn-collision activity forming Kim Boi, Muong Lat, and Sam Son massifs, and ended with post-collision activity forming Nam Rom and Song Ma massifs.

Keywords: Petrology, I-type granite, S-type granite, Indochina, Sino-Vietnam, Geochronology.

1. Introduction

Modern magmatism and tectonic studies consider three geodynamic settings: subduction zone (intra-oceanic arc system or active continental margin - ACM), accretion-collision zones, and large igneous provinces characterized by different series of magmatic

[*]Corresponding author, Email: canpn87@gmail.com

activities and their spatial distribution. They can be concurrent to each other. Thus, it isn't easy to interpret the relationship between geodynamic, magmatic activities, and metallogeny.

The geology of Southeast Asia during the Permian-Triassic period is dominated by two regional events, the amalgamation of Indochina and Sino-Vietnam and the formation of Emeishan Large Igneous Province. The polygon for understanding the Indochina and Sino-Vietnam collision is the Truong Son Fold Belt (TSFB) or Indosinian orogeny. The TSFB (eastern side of Indochina block) and the Loei Fold Belt (Northwest Laos, Southwest Thailand) are the two significant geological structures of the Indochina Composite Terrane. The TSFB is 50 to 250 km wide, >1000 km long, extending from the northeast of Laos to northwest Vietnam and the Tam Ky - Phuoc Son suture zone (north Kontum massif), could be separated into three segments: northwest, central, and southeast (Tran et al., 2008). The Early Paleozoic to Late Paleozoic - Early Mesozoic (Permian-Triassic) granitoids are distributed along the TSFB (primarily concentrated in the northwest segment) with distinct geochemical characteristics (Liu et al., 2012; Roger et al., 2014; Manaka et al., 2014; Shi et al., 2015; Wang et al., 2016). Based on the recent zircon U-Pb dating, the TSFB granitoids were formed in a period of 70 My, from 290 to 220 Ma (Liu et al., 2012; Roger et al., 2014; Zaw et al., 2014; Shi et al., 2015; Hieu et al., 2015, 2017, 2019; Wang et al., 2016). Moreover, different granite types indicated a complicated crustal evolution of the study area. Therefore, there are two remaining questions about (1) the tectonic setting of the TSFB-related granitoids and (2) their geodynamics needed to address.

In this study, we report new data of mineralogy, whole-rock elemental and isotope geochemistry, and geochronology of the Permian-Triassic I- and S-type granites in the Dien Bien - Song Ma Fault zone to clarify their geochemical characteristics, magma sources, and their position in the amalgamation of the Indochina and Sino-Vietnam composite terranes.

2. Geological background

The geology of Northwest Vietnam consists of two major units (Indochina Composite Terrane in the southwest and Sino-Vietnam Composite Terrane in the northeast) and one minor unit (Simao terrane). The Indochina Composite Terrane and the Sino-Vietnam Composite Terrane were amalgamated by the Song Ma suture (Tran et al., 2020; Fig. 1), while a fragment of the Simao Terrane was separated from others by Dien Bien Phu fault (Metcalfe, 2013; Liu et al., 2012; Tran et al., 2020).

The structure of Northwest Vietnam consists of five units: (1) Phan Si Pan uplift including Archean Suoi Chieng metamorphic rocks and Ca Vinh tonalite-trondhjemite complexes, Permian alkaline granitoids, and Cenozoic granitic rocks; (2) Song Da - Tu Le rift with Permian-Triassic basic and felsic volcanogenic rocks and Mesozoic sedimentary rocks; (3) Nam Su Lu - Nam Co subterrane containing garnet-mica schist, garnet amphibolite, and eclogite; (4) Song Ma Ophiolite containing serpentinite, meta-gabbro, metabasalt. (5) Sam Nua - Hoanh Son volcanic belt (Tran and Vu, 2011).

The Permian-Triassic TSFB granitoids can be classified as I-type (Nam Meng, Muong Tung, Nam Rom, Song Ma) and S-type granites (Pu Si Lung, Kim Boi, Muong Lat, and Sam Son) (Fig. 1). The I-type granitic rocks are granodiorite, granite, leucogranite, aplite, pegmatite, alkalic-calcic lamprophyre (kersantite, spessartite), and contain the dioritic xenoliths (sometime gabbro diorite) (Fig. 2A). The S-type granites are major leucocratic biotite and two-mica granite with minor melanocratic granodiorite. Xenoliths of metamorphosed sediment are frequently observed in the S-type granitic rocks (Fig. 2B).

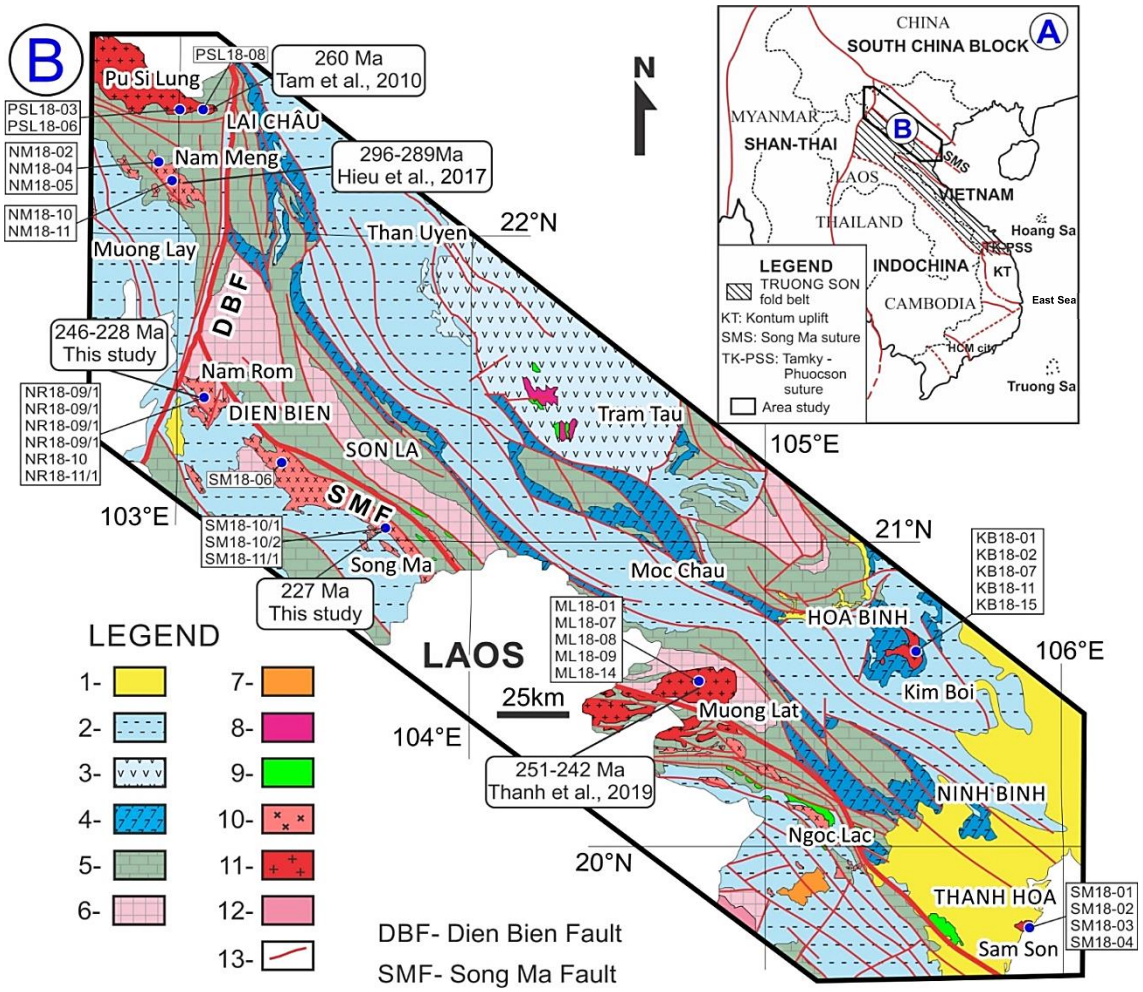

Figure 1. Simplified map showing the distribution of the I-type and S-type granites in the Northwest segment of the TSBF. *Legend:* 1- Cenozoic; 2- Mesozoic (Triassic) volcano-, terrigenous and carbonate formations; 3- Permian rhyolite; 4- Permian flood basalts; 5- Paleozoic formations; 6- Proterozoic metamorphic complexes; 7- Oligocene granite; 8- Permian A-Type Granite; 9- Ultramafic-mafic intrusions; 10- Permian-Triassic I-Type granite; 11- Permian-Triassic S-Type granite; 12- Ordovician granite; 13- fault

3. Methods

3.1. Sampling method

Fifteen samples of the I-type granitic rocks have been collected from Nam Meng (five), Nam Rom (six), and Song Ma (four) massifs. The Nam Meng and Nam Rom massifs are categorized into Dien Bien Complex, while Song Ma is the representative massif of Song Ma Complex (Dovjikov et al., 1965; Dao and Huynh, 1995). Seventeen samples of the S-type granitic rocks have been collected from Kim Boi (five), Muong Lat (five), Pu Si Lung (five), and Sam Son (five) massifs which were categorized into Truong Son Complex (Tri and Vu, 2011).

3.2. Chemical compositions of minerals

The chemical compositions of amphibole and biotite were determined using a JEOL

Superprobe JXA 8230 at the Institute of Geology and Mineralogy, Siberian Branch of the Russian Academy of Sciences (IGM SB-RAS). Measurement conditions and optimizations were described in Pham-Ngoc et al. (2020).

3.3. Whole-rock geochemistry

The whole-rock geochemistry was analyzed by Activation Laboratories (Actlabs) in Ancaster, Ontario, Canada, under Code 4Litho. About 200 g of rock sample were crushed and pulverized at the Institute of Geological Sciences, Vietnam Academy of Science and Technology (IGS VAST). The powdered sample was then equally separated into two parts, sending one portion (about 100 g) to the Actlabs in Ancaster. At the Actlabs, 5 g of powder were mixed with lithium metaborate/ tetraborate and fused. The resulting molten bead is rapidly digested in a weak nitric acid solution to determine major and trace elements using an ICP-OES and an ICP-MS, respectively. Analysis of replicated samples and standards confirmed the quality of data.

3.4. In situ zircon geochronology method

In situ zircon U-Pb dating was carried out at the Department of Earth Sciences, National Taiwan Normal University, using an Agilent 8900 Triple Quadrupole ICP-MS coupled to a Teledyne CETAC Analyte Excite Plus laser-ablation system (Teledyne CETAC, Omaha, NE, US), with a 193 nm ArF excimer laser. The laser's spot size for the analysis is 20 μm in diameter. Nancy 91500 zircon and NIST SRM 610 were used as primary standards for external calibration of U-Pb and Pb-Pb isotope ratios, respectively. Data reduction was conducted offline, using an in-house excel spreadsheet for U-Th-Pb age data reduction (Sakata et al., 2014; Hattori et al., 2017; Obayashi et al., 2017). The isobaric interference of ^{204}Hg on ^{204}Pb was removed using a gas-phase charge transfer reaction with NH_3 gas in the collision/reaction cell (Woods, 2017). To correct the isobaric interference, ^{202}Hg was also monitored. A correction for common Pb was based on the ^{204}Pb method (Stern, 1997) and the model for the common Pb compositions (Stacey and Kramers, 1975).

3.5. Radiogenic isotope method

Sr and Nd were extracted by column separation techniques at the Institute of Earth Sciences, Academia Sinica. Elements were extracted and purified using three-step column separation. Weighted sample powder (~100 mg) was transferred to a Teflon beaker and mixed with HF and HNO_3 (50 drops of each acid), then capped and heated (~100°C) for 24 hours. Subsequently, the solution was dried and then mixed with 2 ml 6N HCl to re-dissolve the samples. This step may be repeated to ensure complete dissolution. After drying, 2 ml of 1N HCl was added to the solute and placed in a centrifuge for 10 minutes; the supernatant was transferred to a new beaker. If there was a residue in the beaker, the dissolution process should be repeated. The final step was to modify the solution from a mixture of HCl and HNO_3 for thermal ionization mass spectrometry (TIMS) analysis to a nitric acid-only phase for multi-collector inductively coupled plasma mass spectrometry (MC-ICP-MS) analysis. The small volume of solute and solution was obtained after the Sr and Nd columns were dried and then mixed with one drop of HNO_3. This step was repeated six times to remove any remaining HCl. After complete dryness, 2 ml 2% HNO_3 was added into the sample beaker and transferred to a solution tube that would be used for analysis on the MC-ICP-MS.

4. Results

4.1. Petrography and Mineralogy

4.1.1. The I-type granites

The I-type granitic rocks vary from gabbro-diorite, diorite, quartz diorite, granodiorite to amphibole-biotite granite (Fig. 2A). The diorite and quartz diorite consists of large amounts of plagioclase (Pl: 50-55%) and K-feldspar (Kfs: 10-15%), lesser amounts of amphibole (Amf: 7-10%), biotite (Bt - 3-5%), and quartz (Qz - 5-15%) and small amounts of sphene, apatite, and titanite (Fig. 2C). Granodiorite and granite have similar mineral assemblages to the diorite with different proportions (Fig. 2D). All minerals are medium to coarse grain size, subhedral, and have the porphyritic texture of Pl and Kfs (5-8 mm). Granophyre texture with the intergrowth of Qz-Kfs could be observed in the Song Ma granodiorite and Bt-Amf granite which indicates a subvolcanic/hypabyssal environment.

The amphibole of Nam Rom granitoid is edenite, while the amphibole in Song Ma pluton is ferro-edenite (Table 1); two amphiboles show a different trend in Al/(Ca+Na+K) - Al/(Na+K) diagram (Pham-Ngoc et al., 2020). The difference in the amphiboles may reflect the difference in the magmatic conditions. Biotite has high MgO (9.10-11.5 wt.%), Mg# = 0.47-0.50, TiO_2 (2.64-3.81wt%) (Table 2), low Al# which indicate a Phlogopite-Annite characteristic ($Phl_{0.43}Sid_{0.29}Ann_{0.28}$).

4.1.2. The S-type granites

The S-type granitic rocks are Bt granite (Pu Si Lung and Kim Boi massifs; Fig. 2E) and two-mica granite (Muong Lat and Sam Son massifs; Figs. 2B, 2F). The S-type granite has a porphyritic texture that contains 5-7 mm Kfs and Pl grains. The essential minerals are Qz (28-30%), Kfs (30-35%), Pl (25-30%), Bt (10-15%), and Ms (5-7%). Biotite and muscovite occur as single grains, sometimes as aggregates. Biotite is partially replaced by secondary muscovite (Figs. 2E, F). The minor minerals are apatite, zircon, sillimanite, and cordierite.

The biotite in Kim Boi granite has high MgO (10.3-11.5 wt.%; Mg# = 0.5), TiO_2 (2.67-3.89 wt.%), Fe (Fe# = 0.48-0.66); Al_2O_3 (15.9-16.9 wt.%), which is similar to the composition of biotite in I-type granite. On the other hand, the biotite of Muong Lat and Sam Son two micas granites are high in TiO_2 (1.83-3.25 wt.%), Al_2O_3 (18.51-20.09 wt.%), and low MgO (4.82-6.77 wt.%). Muscovite is high TiO_2 (0.6-0.9 wt.%), Al_2O_3 (35.49-36.87 wt.%), and F (0.30-0.44 wt.%), and low Mg (0.50-0.73 wt.%) (Table 3).

4.2. Whole-rock geochemistry

4.2.1. The I-type granites

The SiO_2 contents in the I-type granitic rocks vary from low in the gabbro-diorite and dioritic xenoliths (in granodiorite and Bt-Amf granite) (52.4-59.7 wt.%) to high in the Song Ma Bt-Amf granite (71.1 wt%). The magma are low in Al_2O_3 (14-16 wt.%), high alkali (Na_2O+K_2O = 4.73-9.21 wt.%, mostly 6-7.5 wt.%; K/Na = 0.1-0.7) (Table 4, Fig. 3). The alkali in the granitoid of the Nam Rom massifs is higher than of the Nam Meng and Song Ma massifs. In which, Song Ma pluton has higher concentrations of Na than K, similar to the rhyolitic rocks in the Song Ma suture zone (Tran et al., 2008). The rocks are calk-alkaline to shoshonite (Fig. 4), the ASI (A/CNK) varies from 0.64-1.14, reflecting a metaluminous to relatively peraluminous I-type granite (Fig. 5). The I-type granitic rocks are rich in Rb (67-180 ppm), Sr (59-1,660 ppm, mostly 134-390 ppm), Ba (132-3,114 ppm, mostly 300-700 ppm), Zr (64-170 ppm) (Table 4). The K/Rb, Rb/Sr, and Rb/Ba ratios are 179-334, 0.40-3.50, and 0.16-0.38, respectively. They are also rich in rare earth elements (ΣREE = 78-563 ppm), especially the

LREE, and low in HREE, depleted in Eu with the Eu/Eu*= 0.50-0.96. The ratios of $[La/Sm]_N$, $[La/Yb]_N$, and $[Gd/Yb]_N$ varies from a range of 1.08-4.92, 1.57-27.33, and 1.07-3.72, respectively (Fig. 6A). The rocks are rich in Rb, Ba, Zr, Th, U, La, Ce, but low in Ti, Nb, and Ta, identical to the I-granite in the subduction zone (Fig. 6B).

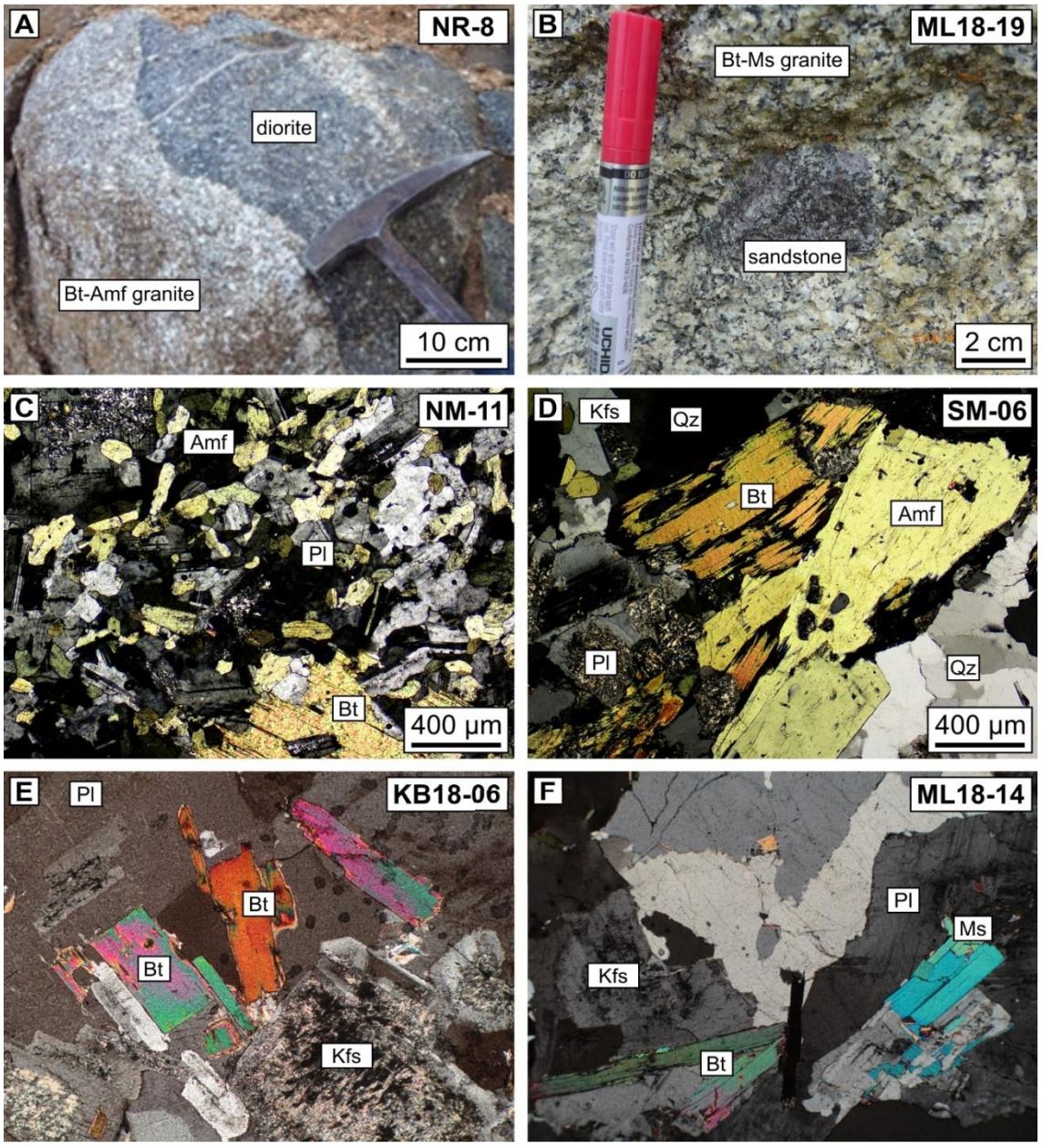

Figure 2. Photographs and photomicrographs of the Permian-Triassic granitoids. A - Diorite xenolith in Bt-Amf granite; B - Sandstone xenolith in granite; C - Nam Meng fine-grained diorite; D - Song Ma Bt-Amf granite; E - Kim Boi Bt granite; F - Muong Lat two micas (Bt-Ms) granite. Sample: NR - Nam Rom; ML - Muong Lat; NM - Nam Meng; SM - Song Ma; KB - Kim Boi. Minerals: Amf - amphibole; Bt - biotite; Ms - Muscovite; Pl - plagioclase; Kfs - potassium feldspar; Qz - quartz

Table 1. Chemical compositions (wt.%) of amphibole in the Nam Rom (NR) and Song Ma (SM) granitoids

Sample	NR-11/1										
Point	1	2	3	4	5	6	9	10	12	13	15
SiO_2	43.71	42.75	43.84	46.62	42.70	44.07	43.86	42.27	44.29	43.42	43.60
TiO_2	1.31	1.23	1.21	0.92	1.29	1.15	1.23	1.32	1.14	1.24	1.25
Al_2O_3	9.77	9.52	9.24	7.28	9.77	8.67	9.24	9.72	8.71	9.36	9.68
FeO	18.28	18.08	17.92	17.20	18.25	17.92	17.83	18.35	17.78	17.77	18.17
MgO	10.18	10.33	10.69	11.68	10.07	10.64	10.45	10.11	10.74	10.59	10.20
MnO	0.44	0.47	0.43	0.47	0.48	0.48	0.47	0.47	0.48	0.46	0.48
BaO	0.03	0.001	0.018	0.00	0.00	0.00	0.00	0.031	0.006	0.00	0.028
CaO	11.55	11.52	11.50	11.62	11.53	11.49	11.45	11.49	11.56	11.48	11.45
Na_2O	1.59	1.66	1.62	1.18	1.70	1.47	1.59	1.55	1.39	1.47	1.67
K_2O	1.32	1.22	1.16	0.77	1.30	1.06	1.18	1.28	1.03	1.16	1.23
F	0.38	0.42	0.38	0.36	0.45	0.31	0.39	0.41	0.41	0.31	0.30
Cl	0.19	0.19	0.16	0.09	0.20	0.14	0.12	0.17	0.13	0.14	0.19
Total	*98.74*	*97.38*	*98.15*	*98.20*	*97.74*	*97.40*	*97.81*	*97.17*	*97.66*	*97.38*	*98.24*

Table 1 (cont.)

Sample	SM-11/1										
Point	2	3	5	7	9	10	11	12	15	22	24
SiO_2	45.10	44.54	44.18	44.46	44.52	44.14	45.20	44.06	44.30	44.18	43.97
TiO_2	1.38	1.62	1.61	1.48	1.66	1.55	1.21	1.70	1.57	1.68	1.37
Al_2O_3	6.24	6.69	7.01	6.74	6.80	6.76	5.88	6.98	6.87	6.96	6.54
FeO	27.07	26.45	26.65	25.98	26.03	26.28	24.99	25.85	25.91	26.28	26.55
MgO	5.78	6.39	5.84	6.24	6.36	6.31	7.33	6.42	6.40	6.00	5.96
MnO	0.50	0.38	0.50	0.46	0.54	0.49	0.61	0.55	0.54	0.51	0.64
BaO	0.00	0.008	0.043	0.00	0.046	0.00	0.00	0.013	0.021	0.00	0.005
CaO	9.23	9.59	9.73	9.87	9.73	9.56	9.70	9.83	9.76	9.81	9.56
Na_2O	2.24	2.20	2.44	2.34	2.31	2.36	2.05	2.43	2.49	2.34	2.18
K_2O	0.59	0.47	0.62	0.51	0.62	0.56	0.72	0.54	0.49	0.55	0.78
F	0.84	0.87	0.86	0.75	0.82	0.90	0.83	0.79	0.90	0.74	0.54
Cl	0.25	0.27	0.33	0.31	0.33	0.30	0.39	0.32	0.28	0.33	0.44
Total	*99.21*	*99.49*	*99.80*	*99.14*	*99.75*	*99.22*	*98.90*	*99.47*	*99.53*	*99.36*	*98.54*

Table 2. Chemical compositions (wt.%) of biotite in the I-type and S-type granitoids

Sample	NR-9/3								SM-11/1
Point	1	3	4	12	13	14	15	16	21
SiO_2	36.31	36.49	35.90	36.12	35.81	35.64	35.87	37.48	37.51
TiO_2	2.64	3.65	2.97	3.07	2.68	3.17	3.19	2.95	3.81
Al_2O_3	16.10	16.57	16.72	16.01	17.36	16.72	16.73	17.97	11.57
FeO	19.73	19.76	19.75	19.45	19.71	19.67	19.96	18.79	26.33
MgO	8.75	8.13	8.52	9.41	8.59	8.98	8.73	7.74	7.61
MnO	0.33	0.29	0.36	0.34	0.34	0.34	0.32	0.23	0.24
BaO	0.13	0.14	0.12	0.08	0.08	0.06	0.06	0.11	0.00
CaO	0.00	0.03	0.00	0.00	0.00	0.00	0.00	0.00	0.16
Na_2O	0.17	0.13	0.22	0.15	0.16	0.23	0.17	0.20	0.15
K_2O	8.94	8.67	8.84	8.72	8.84	8.96	8.80	8.89	8.42
F	0.71	0.47	0.56	0.71	0.73	0.57	0.73	0.63	0.57
Cl	0.12	0.11	0.10	0.10	0.12	0.09	0.10	0.08	0.52
Total	*93.10*	*93.84*	*93.40*	*93.36*	*93.58*	*93.76*	*93.83*	*94.36*	*95.80*

Table 2 (cont.)

Sample	KB18-06 (Kim Boi)									
Point	1	2	3	4	5	6	7	8	9	10
SiO_2	36.55	36.26	34.36	35.65	36.35	35.78	36.59	33.97	36.37	34.91
TiO_2	3.52	3.44	3.01	3.26	3.74	3.16	3.47	2.67	3.57	3.02
Al_2O_3	16.02	15.98	16.47	16.33	15.85	16.29	16.37	16.85	15.99	16.78
FeO	0.07	0.10	0.25	0.11	0.08	0.32	0.07	0.39	0.04	0.08
MgO	19.21	18.83	20.72	19.75	19.39	19.92	19.42	22.10	19.25	20.16
MnO	0.26	0.22	0.22	0.20	0.17	0.22	0.22	0.24	0.24	0.27
BaO	10.77	10.60	10.78	10.59	10.57	10.92	10.73	11.45	10.63	11.15
CaO	0.00	0.02	0.02	0.01	0.00	0.04	0.00	0.10	0.00	0.05
Na_2O	0.23	0.21	0.23	0.22	0.21	0.22	0.22	0.17	0.19	0.21
K_2O	9.36	9.19	7.42	8.73	9.11	8.25	9.20	5.64	9.41	7.23
F	0.86	0.79	0.54	0.56	0.67	0.54	0.81	0.38	0.79	0.47
Cl	0.16	0.17	0.14	0.15	0.18	0.14	0.18	0.13	0.12	0.14
Total	*97.01*	*95.81*	*94.17*	*95.55*	*96.32*	*95.79*	*97.29*	*94.09*	*96.61*	*94.47*

Table 2 (cont.)

Sample	KB18-06 (Kim Boi)									
Point	11	12	13	14	15	16	17	18	19	20
SiO_2	36.61	35.78	36.49	36.42	35.99	35.65	36.45	36.60	36.46	36.16
TiO_2	3.52	3.51	3.28	3.40	3.41	3.53	3.89	3.88	3.30	3.67
Al_2O_3	16.47	16.81	15.96	16.11	16.07	16.40	15.84	16.73	16.01	16.84
FeO	0.08	0.05	0.06	0.07	0.07	0.06	0.05	0.05	0.11	0.12
MgO	19.19	19.54	19.38	18.89	18.97	18.85	19.24	17.99	18.79	19.35
MnO	0.23	0.20	0.20	0.19	0.28	0.18	0.11	0.14	0.20	0.21
BaO	10.51	10.60	11.02	10.77	10.44	10.24	10.58	10.12	10.66	10.27
CaO	0.00	0.00	0.01	0.00	0.00	0.01	0.00	0.00	0.00	0.00
Na_2O	0.21	0.24	0.18	0.22	0.25	0.22	0.24	0.22	0.25	0.22
K_2O	9.19	8.62	8.80	9.40	9.06	9.18	9.13	9.41	9.10	9.04
F	0.75	0.57	0.59	0.66	0.85	0.75	0.72	0.72	1.02	0.58
Cl	0.15	0.19	0.18	0.16	0.10	0.15	0.16	0.16	0.16	0.20
Total	*96.91*	*96.12*	*96.15*	*96.30*	*95.49*	*95.22*	*96.41*	*96.04*	*96.07*	*96.66*

Table 2 (cont.)

Sample	KB18-06 (Kim Boi)						ML18-14 (Muong Lat)			
Point	21	22	23	24	25	26	1	2	3	4
SiO_2	36.03	35.58	36.21	36.31	35.74	36.14	34.42	34.40	33.98	34.28
TiO_2	3.17	3.51	3.35	3.33	2.96	3.29	2.63	2.50	3.28	2.43
Al_2O_3	16.72	16.81	16.13	16.36	16.24	16.18	18.99	18.91	17.85	19.42
FeO	0.06	0.10	0.05	0.07	0.10	0.07	0.01	0.14	0.03	0.01
MgO	19.71	20.16	19.27	19.40	20.78	20.15	22.84	21.89	22.92	22.19
MnO	0.16	0.20	0.22	0.20	0.25	0.24	0.47	0.48	0.43	0.50
BaO	10.67	10.51	11.08	10.50	11.35	10.89	5.80	5.59	5.63	5.90
CaO	0.01	0.01	0.01	0.02	0.03	0.05	0.01	0.04	0.02	0.00
Na_2O	0.23	0.17	0.19	0.20	0.19	0.21	0.12	0.16	0.03	0.07
K_2O	8.99	8.43	8.84	9.24	7.43	8.54	9.55	9.43	9.39	9.59
F	0.63	0.50	0.73	0.76	0.51	0.57	1.07	1.04	1.07	1.05
Cl	0.17	0.15	0.16	0.18	0.14	0.15	0.01	0.02	0.01	0.01
Total	*96.57*	*96.14*	*96.23*	*96.57*	*95.71*	*96.47*	*95.91*	*94.60*	*94.63*	*95.45*

Table 2 (cont.)

Sample	ML18-14 (Muong Lat)									
Point	5	6	7	8	9	10	11	12	13	14
SiO_2	35.10	34.55	30.37	34.83	35.37	35.55	35.60	34.61	35.17	34.99
TiO_2	2.95	3.12	1.72	2.63	2.70	2.78	3.33	2.87	2.82	2.60
Al_2O_3	19.48	19.61	20.23	19.58	19.47	20.10	20.11	19.16	18.81	19.45
FeO	0.01	0.01	0.01	0.02	0.01	0.02	0.02	0.00	0.03	0.01
MgO	22.44	20.87	26.72	22.47	21.49	20.97	21.34	22.30	22.14	22.36
MnO	0.47	0.50	0.63	0.47	0.48	0.46	0.49	0.46	0.47	0.48
BaO	5.74	5.79	6.68	6.11	6.00	6.02	5.19	6.08	5.99	6.02
CaO	0.01	0.00	0.01	0.00	0.00	0.00	0.00	0.00	0.00	0.00
Na_2O	0.06	0.13	0.02	0.07	0.09	0.12	0.09	0.08	0.10	0.10
K_2O	9.69	9.57	4.99	9.38	9.71	9.44	9.93	9.48	9.71	9.54
F	1.07	1.21	0.67	1.04	0.99	1.11	0.77	0.99	1.00	1.00
Cl	0.01	0.01	0.00	0.01	0.00	0.01	0.02	0.01	0.01	0.01
Total	*97.04*	*95.37*	*92.04*	*96.63*	*96.31*	*96.60*	*96.87*	*96.04*	*96.25*	*96.56*

Table 2 (cont.)

Sample	ML18-14 (Muong Lat)									
Point	15	16	17	18	19	20	21	22	23	24
SiO_2	35.14	34.58	35.53	33.82	35.61	35.62	35.18	35.42	35.20	34.78
TiO_2	1.83	2.92	2.66	3.25	2.62	2.34	2.08	2.52	2.33	2.56
Al_2O_3	19.77	19.15	19.31	18.51	19.68	19.07	19.92	19.80	19.10	19.48
FeO	0.00	0.02	0.10	0.07	0.01	0.03	0.03	0.07	0.03	0.02
MgO	21.71	22.46	22.32	24.25	22.27	21.86	21.38	21.18	21.79	21.68
MnO	0.49	0.56	0.54	0.54	0.47	0.48	0.43	0.47	0.46	0.46
BaO	6.24	5.62	5.68	5.57	6.06	6.77	6.27	6.06	6.38	6.02
CaO	0.01	0.00	0.01	0.01	0.00	0.00	0.00	0.02	0.00	0.00
Na_2O	0.11	0.15	0.09	0.07	0.16	0.11	0.17	0.20	0.09	0.11
K_2O	9.78	9.49	9.66	8.99	9.51	9.52	9.50	9.52	9.81	9.72
F	1.06	0.91	1.08	0.84	1.11	1.08	1.20	1.05	1.14	1.05
Cl	0.01	0.01	0.01	0.02	0.01	0.01	0.02	0.01	0.01	0.01
Total	*96.15*	*95.86*	*96.98*	*95.95*	*97.51*	*96.90*	*96.17*	*96.35*	*96.33*	*95.90*

Table 2 (cont.)

Sample	ML18-14 (Muong Lat)									
Point	25	26	27	28	29	30	31	32	33	34
SiO_2	35.55	34.64	35.34	35.18	34.50	34.70	35.43	35.04	35.22	35.27
TiO_2	2.43	3.03	2.68	2.52	3.62	3.51	2.98	2.95	2.60	2.85
Al_2O_3	20.09	18.81	19.80	19.48	18.56	18.97	19.53	19.73	20.01	19.64
FeO	0.27	0.03	0.01	0.06	0.10	0.04	0.03	0.00	0.00	0.02
MgO	21.07	22.57	21.57	21.40	22.03	21.05	21.78	21.66	20.35	21.94
MnO	0.46	0.48	0.49	0.47	0.53	0.50	0.48	0.50	0.41	0.47
BaO	5.89	6.06	6.05	5.83	5.67	5.32	6.04	5.98	5.94	5.90
CaO	0.03	0.02	0.02	0.03	0.02	0.00	0.00	0.00	0.00	0.00
Na_2O	0.14	0.11	0.21	0.12	0.18	0.06	0.10	0.09	0.07	0.18
K_2O	9.37	9.69	9.48	9.61	9.51	9.54	9.60	9.70	9.74	9.56
F	0.98	1.02	0.99	0.84	0.91	0.88	1.16	1.00	0.95	1.14
Cl	0.02	0.01	0.01	0.01	0.01	0.01	0.01	0.01	0.01	0.01
Total	*96.29*	*96.47*	*96.66*	*95.54*	*95.62*	*94.57*	*97.14*	*96.65*	*95.30*	*96.98*

Table 2 (cont.)

Sample	ML18-14 (Muong Lat)						SS18-02 (Sam Son)				
Point	35	36	37	38	39	40	1	2	3	4	5
SiO_2	35.16	34.94	34.85	35.14	34.56	34.38	34.41	33.80	34.30	34.26	33.70
TiO_2	2.43	2.70	2.85	2.73	2.49	3.03	2.30	2.39	2.39	2.31	2.17
Al_2O_3	19.31	19.03	19.43	19.11	19.93	18.77	19.05	19.00	19.10	18.74	19.18
FeO	0.01	0.03	0.04	0.02	0.01	0.02	0.01	0.02	0.00	0.02	0.02
MgO	22.48	21.98	22.62	22.89	21.58	24.05	22.63	23.06	22.79	23.42	23.28
MnO	0.48	0.46	0.50	0.48	0.53	0.61	0.56	0.61	0.56	0.61	0.59
BaO	6.15	6.15	5.82	6.13	5.53	5.27	5.09	4.82	5.06	5.03	4.89
CaO	0.00	0.00	0.01	0.00	0.00	0.04	0.01	0.01	0.00	0.01	0.03
Na_2O	0.10	0.05	0.19	0.16	0.08	0.03	0.06	0.09	0.03	0.02	0.10
K_2O	9.68	9.64	9.43	9.53	9.86	9.32	9.60	9.64	9.31	9.25	9.41
F	1.05	1.01	1.11	0.91	0.87	0.86	0.77	0.74	0.62	0.50	0.69
Cl	0.01	0.01	0.01	0.00	0.01	0.01	0.01	0.01	0.00	0.01	0.00
Total	*96.85*	*95.99*	*96.84*	*97.11*	*95.45*	*96.40*	*94.49*	*94.18*	*94.18*	*94.18*	*94.06*

Table 3. Chemical compositions (wt.%) of muscovite in the Muong Lat and Sam Son granitoids

Sample	ML18-14 (Muong Lat)										
Point	1	2	3	4	5	6	7	8	9	10	11
SiO_2	47.47	46.98	47.36	47.58	47.73	46.54	47.51	47.68	47.58	47.27	47.14
TiO_2	0.64	0.99	0.64	0.74	0.91	0.75	1.30	0.17	0.73	0.62	0.63
Al_2O_3	36.87	35.85	36.10	35.85	35.90	35.61	35.96	36.39	35.93	35.49	35.87
FeO	0.01	0.01	0.03	0.01	0.02	0.04	0.02	0.04	0.01	0.01	0.03
MgO	0.68	0.85	1.19	1.18	1.17	1.06	1.16	1.17	1.20	1.17	1.17
MnO	0.02	0.00	0.03	0.01	0.02	0.02	0.01	0.03	0.02	0.01	0.02
BaO	0.50	0.54	0.71	0.73	0.68	0.69	0.67	0.71	0.68	0.72	0.63
CaO	0.00	0.00	0.00	0.00	0.00	0.00	0.00	0.01	0.00	0.00	0.01
Na_2O	0.42	0.48	0.69	0.71	0.66	0.50	0.51	0.67	0.56	0.52	0.67
K_2O	10.91	10.80	10.50	10.46	10.57	10.73	10.67	10.49	10.66	10.73	10.39
F	0.35	0.33	0.39	0.42	0.41	0.40	0.42	0.40	0.44	0.43	0.41
Cl	0.00	0.00	0.00	0.01	0.01	0.00	0.00	0.00	0.01	0.00	0.01
Total	*97.88*	*96.84*	*97.63*	*97.70*	*98.06*	*96.35*	*98.24*	*97.75*	*97.82*	*96.97*	*96.98*

Table 3 (cont.)

Sample	ML18-14 (Muong Lat)					SS18-02 (Sam Son)					
Point	1	2	3	4	5	1	2	3	4	5	6
SiO_2	47.47	46.98	47.36	47.58	47.73	46.54	47.51	47.68	47.58	47.27	47.14
TiO_2	0.64	0.99	0.64	0.74	0.91	0.75	1.30	0.17	0.73	0.62	0.63
Al_2O_3	36.87	35.85	36.10	35.85	35.90	35.61	35.96	36.39	35.93	35.49	35.87
FeO	0.01	0.01	0.03	0.01	0.02	0.04	0.02	0.04	0.01	0.01	0.03
MgO	0.68	0.85	1.19	1.18	1.17	1.06	1.16	1.17	1.20	1.17	1.17
MnO	0.02	0.00	0.03	0.01	0.02	0.02	0.01	0.03	0.02	0.01	0.02
BaO	0.50	0.54	0.71	0.73	0.68	0.69	0.67	0.71	0.68	0.72	0.63
CaO	0.00	0.00	0.00	0.00	0.00	0.00	0.00	0.01	0.00	0.00	0.01
Na_2O	0.42	0.48	0.69	0.71	0.66	0.50	0.51	0.67	0.56	0.52	0.67
K_2O	10.91	10.80	10.50	10.46	10.57	10.73	10.67	10.49	10.66	10.73	10.39
F	0.35	0.33	0.39	0.42	0.41	0.40	0.42	0.40	0.44	0.43	0.41
Cl	0.00	0.00	0.00	0.01	0.01	0.00	0.00	0.00	0.01	0.00	0.01
Total	*97.88*	*96.84*	*97.63*	*97.70*	*98.06*	*96.35*	*98.24*	*97.75*	*97.82*	*96.97*	*96.98*

Table 4. Whole-rock geochemistry of the I-type and S-type granites in TSBF

Sample	NM02	NM04	NM05	NM10	NM11	NR8	NR9/1	NR9/3
Rock type	GBD	GBD	GND	GND	GBD	GND	BAG	GND
SiO_2 (wt.%)	52.84	54.68	63.61	64.4	52.38	66.06	69.46	67.14
TiO_2	0.65	0.73	0.44	0.47	0.79	0.37	0.29	0.4
Al_2O_3	18.83	19.44	16.32	16.02	18.94	15.42	15.32	14.58
Fe_2O_3(T)	10.15	8.27	5.52	5.39	9.91	3.47	2.28	3.24
MnO	0.32	0.24	0.13	0.12	0.24	0.07	0.08	0.06
MgO	3.42	2.83	1.87	1.92	3.42	1.51	1.04	1.7
CaO	7.33	7.35	5.44	5.19	7.49	2.73	1.24	2.68
Na_2O	3.51	4.12	3.44	3.31	3.98	3.74	3.49	2.96
K_2O	1.95	1.65	1.49	1.94	1.77	3.85	5.08	5.01
P_2O_5	0.13	0.16	0.13	0.12	0.16	0.14	0.18	0.11
LOI	1.25	0.92	1.22	0.77	1.06	2.38	1.12	1.82
Total	*100.4*	*100.4*	*99.59*	*99.65*	*100.1*	*99.74*	*99.58*	*99.7*
Rb (ppm)	62	56	53	70	67	110	235	139.3
Cs	2.2	2.1	1.2	1.6	1.4	7.8	20.2	3
Be	1	1	< 1	< 1	1	4.3	5	3.9
Sr	268	317	273	251	285	336	134.2	1660
Ba	387	368	337	399	323	785	400.8	3114
Sc	22	14	7	8	17	9.6	5.5	24.2
Zr	73	89	146	117	113	153	94.6	170.8
Hf	2.6	2.8	3.7	3.1	3	2.6	2.9	3.4
Nb	8	9	5	5	5	11.9	16.3	29.8
Ta	0.8	0.7	0.4	0.5	0.4	1.7	2.6	1.3
Y	43	30	15	16	27	13.3	12.1	21.5
La	12.5	17.1	22.4	12.8	14.8	38.6	14.9	151.4
Ce	32.7	44.2	39.2	26.4	36.1	72.8	35.5	264.6
Pr	5.2	6.4	4.2	3.3	4.9	7.7	4.1	25.8
Nd	25.7	28	14.5	12.8	21	27.4	15.3	86
Sm	7.5	6.7	3.1	2.9	5.2	5.1	3.5	12.1
Eu	1.6	1.6	0.9	0.9	1.4	1	0.6	3.3
Gd	7.4	6.1	2.8	2.8	5	4.6	3.2	10
Tb	1.3	1	0.5	0.5	0.8	0.6	0.5	1
Dy	8.2	6.4	3	3	5.6	2.9	2.4	4.2
Ho	1.6	1.2	0.6	0.6	1.1	0.5	0.4	0.7
Er	5.1	3.9	1.9	1.9	3.4	1.4	1.1	1.8
Tm	0.8	0.6	0.3	0.3	0.5	0.2	0.2	0.2
Yb	5.7	4.4	1.9	2.1	3.5	1	1.1	1.6
Lu	0.9	0.7	0.3	0.3	0.5	0.2	0.2	0.2
V	118	91	65	73	185	99	26.8	224.4
Cr	20	< 20	< 20	< 20	< 20	18.1	7.6	62
Co	15	14	10	10	19	7	4	29.3
Ni	20	< 20	< 20	< 20	< 20	6.7	3.3	23.7
Cu	10	< 10	< 10	< 10	60	2.2	1.7	10
Zn	110	90	60	60	90	62.6	36.8	78.8
Pb	6	6	< 5	< 5	< 5	31.6	71.8	22.2
Ga	19	20	16	16	19	18.4	26.7	65.4
Ge	3	2	1	2	2		1.2	2.1
Th	3.4	5	8	7.3	2.6	17.3	11.3	33.7
U	1.8	1.3	1.5	1.8	0.7	2.5	9.7	4.1

Table 4 (cont.)

Sample	NR9/4	NR9/5	NR11/1	SM6	SM 10/1	SM 10/2	SM 11/1	KB18-01
Rock type	QD	BAG	QD	GND	BAG	QD	BAG	BG
SiO_2 (wt.%)	63.94	68.63	61.94	62.36	67.08	64.12	71.07	70.2
TiO_2	0.44	0.3	0.65	0.53	0.46	0.67	0.39	0.32
Al_2O_3	15.91	15.11	16.2	16.53	14.07	14.76	13.81	14.4
Fe_2O_3(T)	4	2.65	5.42	4.97	4.85	6.91	4.34	2.56
MnO	0.08	0.03	0.1	0.09	0.08	0.09	0.08	0.06
MgO	2.62	1.43	3.09	2.68	1.11	2.15	0.47	1.04
CaO	3.31	1.41	2.62	4.8	2.73	3.17	2.6	1.51
Na_2O	3.42	3.24	3.74	3.09	5.85	5.26	3.93	2.78
K_2O	3.84	4.94	3.8	3.49	0.65	1.08	1.97	4.28
P_2O_5	0.12	0.15	0.19	0.17	0.13	0.19	0.08	0.19
LOI	1.95	1.87	2.16	1.13	2.66	1.42	1.05	1.41
Total	*99.63*	*99.76*	*99.91*	*99.84*	*99.67*	*99.82*	*99.79*	*98.74*
Rb (ppm)	142.9	180.2	149	92	16.1	29.1	78	274
Cs	8.5	10.1	10.6	6.1	0.5	0.5	1	22.3
Be	4.4	5.3	5.6	4.1	1.3	1.7	1.8	3
Sr	378.4	184.6	353	417	67.8	187.3	176	88
Ba	1236	659.7	951	848	132.9	287.3	479	280
Sc	18.9	5.7	16.5	13.9	12.8	17.8	10.7	6
Zr	90.8	131.1	195	166	140.5	85.3	123	100
Hf	2.3	3.5	1.7	1.6	3.7	2.1	2	3
Nb	12.4	13.4	11.9	12.9	12	6.5	9.2	9
Ta	0.6	1.2	4.1	2.8	0.9	0.4	1.5	1.9
Y	17.8	12.3	25.1	17.7	37.2	20.8	25.7	14
La	31.3	18.6	45.1	55.3	29.8	14.4	20.7	25.2
Ce	64.4	41.9	87.3	100.1	61.9	30.5	41.9	53.5
Pr	6.8	5.2	9.5	10.2	7.2	3.6	4.9	6.1
Nd	24.9	19.6	36.2	36.1	26.4	13.9	19.5	22.6
Sm	5	4.5	6.6	6.1	5.4	3	4.1	5.3
Eu	1.2	0.8	1.4	1.2	0.9	0.9	0.9	0.7
Gd	4.7	3.9	6.4	5.5	5.5	3.2	4.8	4.3
Tb	0.7	0.5	0.8	0.6	0.9	0.5	0.7	0.6
Dy	3.6	2.7	4.7	3.3	5.3	3.1	4.3	3.6
Ho	0.7	0.5	0.9	0.7	1.1	0.7	0.9	0.6
Er	1.8	1.2	2.6	1.9	3.4	2	2.7	1.7
Tm	0.2	0.2	0.4	0.3	0.5	0.3	0.4	0.3
Yb	1.4	1.1	2.4	1.6	3.6	2	2.6	1.7
Lu	0.2	0.2	0.4	0.3	0.5	0.3	0.4	0.3
V	63.1	34.5	165	105	25.7	73.1	20.7	26
Cr	16.3	11.5	38	26	1.2	0.8	0	30
Co	7.2	4.5	14.3	12.2	5.1	9.2	4.7	6
Ni	6.4	4.6	13.1	8.4	1.3	1.1	0.9	< 20
Cu	3	3.2	21.9	5.1	2.8	2.4	7.6	< 10
Zn	50.5	49.2	92.1	64	30.5	46.4	64.1	70
Pb	29.1	45.3	24.3	44.7	4.5	1.9	6.7	30
Ga	37.7	31.4	21.1	19.1	18.5	20.4	15.6	19
Ge	1.2	1.2			1.1	1.6		3
Th	15.3	14.6	25.3	28.1	9.1	4.1	6.8	13.2
U	1.8	4.2	6.7	6	1.8	0.9	1.7	8.8

Table 4 (cont.)

Sample	KB18-02	KB18-07	KB18-11	KB18-15	ML18-01	ML18-07	ML18-08	ML18-09
Rock type	BG	BG	GND	GND	BMG	BMG	BMG	BMG
SiO_2 (wt.%)	70.81	69.84	66.93	66.66	72.26	72.99	72.09	72.66
TiO_2	0.29	0.43	0.46	0.65	0.21	0.21	0.19	0.2
Al_2O_3	14.74	13.61	14.86	15.33	13.91	14.11	13.85	13.8
Fe_2O_3(T)	2.25	3.09	3.29	4.53	1.93	1.85	1.78	1.7
MnO	0.05	0.06	0.05	0.07	0.05	0.05	0.05	0.04
MgO	1.02	1.29	1.65	1.87	0.47	0.46	0.44	0.42
CaO	1.4	1.25	2.3	2.15	0.94	0.96	0.9	1.01
Na_2O	2.88	2.39	2.83	2.43	3.04	3.04	3.21	3.06
K_2O	4.34	4.98	4.33	3.83	4.58	4.61	4.63	4.77
P_2O_5	0.21	0.17	0.16	0.16	0.2	0.2	0.22	0.2
LOI	1.42	1.54	1.52	2	0.94	0.82	1.16	0.92
Total	*99.4*	*98.64*	*98.39*	*99.67*	*98.53*	*99.3*	98.51	98.78
Rb (ppm)	270	219	219	196	288	301	302	283
Cs	19.7	12.4	11.9	11	24.2	24.2	28.5	28.9
Be	8	3	4	3	8	8	6	6
Sr	125	189	150	126	86	86	63	69
Ba	366	555	512	498	343	344	308	373
Sc	5	8	8	11	4	4	3	3
Zr	110	131	133	184	92	108	87	95
Hf	3	3.5	3.5	4.8	2.6	3	2.5	2.8
Nb	9	6	7	9	10	13	10	10
Ta	1.5	1.1	1.3	1.2	2	2.2	2.5	2.2
Y	15	22	16	22	13	14	12	15
La	30.1	33.3	32.9	39.6	25.1	25.7	23.3	29.7
Ce	62	69	68.7	82.6	51.3	52.5	47.7	61.3
Pr	7	7.9	7.8	9.4	5.8	5.9	5.4	6.9
Nd	26.1	29.1	29.2	34.6	21	20.8	19.3	24.5
Sm	5.9	6.3	6.1	7.3	4.9	4.8	4.5	5.6
Eu	0.8	1	1	1.1	0.6	0.7	0.6	0.7
Gd	4.7	5.1	4.7	5.6	3.7	3.9	3.6	4.3
Tb	0.6	0.8	0.7	0.8	0.6	0.6	0.5	0.7
Dy	3.1	4.5	3.8	4.8	3	2.9	2.8	3.4
Ho	0.5	0.8	0.7	0.9	0.5	0.5	0.5	0.6
Er	1.4	2.4	2	2.6	1.3	1.3	1.2	1.5
Tm	0.2	0.3	0.3	0.4	0.2	0.2	0.2	0.2
Yb	1.2	2.3	1.9	2.5	1.2	1.1	1.2	1.4
Lu	0.2	0.3	0.3	0.4	0.2	0.2	0.2	0.2
V	24	35	36	57	12	12	9	11
Cr	30	40	50	60	< 20	< 20	< 20	< 20
Co	4	7	7	10	2	3	2	2
Ni	< 20	20	30	30	< 20	< 20	< 20	< 20
Cu	< 10	10	20	20	< 10	< 10	< 10	< 10
Zn	80	90	60	80	60	70	60	60
Pb	57	36	33	29	42	43	43	43
Ga	22	17	18	19	19	21	19	19
Ge	2	2	2	2	2	2	2	2
Th	15.2	14.4	14.1	15.9	14.1	15.2	13.3	17
U	6.5	4.5	4.2	4.4	9.4	10.6	7.9	7.1

Table 4 (cont.)

Sample	ML18-14	PSL03	PSL06	PSL08	SS18-01	SS18-02	SS18-03	SS18-04
Rock type	BMG	GND	BG	GND	BMG	BMG	BMG	BMG
SiO_2 (wt.%)	72.61	64.79	70.37	64.5	73.16	72.09	68.87	72.95
TiO_2	0.2	0.61	0.23	0.69	0.07	0.13	0.6	0.07
Al_2O_3	13.85	15.85	15.31	15.51	14.4	15.24	16.29	14.82
Fe_2O_3(T)	1.75	5.53	2.56	5.35	1.16	1.23	3.95	0.83
MnO	0.05	0.08	0.06	0.08	0.05	0.03	0.11	0.02
MgO	0.45	1.79	0.66	1.84	0.17	0.28	0.94	0.2
CaO	0.97	3.08	1.99	4.46	0.63	0.81	0.67	0.54
Na_2O	2.99	2.71	3.72	2.43	3.39	3.44	2.5	3.26
K_2O	4.71	2.87	2.85	2.77	4.96	4.75	3.36	4.55
P_2O_5	0.2	0.13	0.05	0.16	0.22	0.19	0.07	0.2
LOI	0.74	2.03	1.4	1.96	1.07	0.85	2.07	1.31
Total	98.52	99.46	99.2	99.74	99.26	99.05	99.43	98.76
Rb (ppm)	288	105	86	96	338	258	221	247
Cs	27	1.8	1.9	1.8	34.2	44.2	22.9	30.3
Be	6	3	2	2	6	14	2	11
Sr	63	234	320	243	23	84	131	67
Ba	325	601	566	582	99	569	769	186
Sc	3	15	4	16	3	3	12	2
Zr	88	159	100	165	41	64	194	31
Hf	2.6	4	3.1	4.2	1.6	2	5.5	1.1
Nb	10	11	8	9	13	7	11	6
Ta	2.2	1	0.9	0.8	4.3	2.1	0.8	1.8
Y	13	17	15	21	11	18	31	10
La	24.1	18.4	31.4	33.6	11.4	21.6	31.4	6.7
Ce	49.8	35.4	60.4	67.1	25.3	44.8	67	13.9
Pr	5.6	4.2	6.8	7.6	2.9	5	7.9	1.7
Nd	20.2	16.4	24.5	28.3	10.2	18.4	31.1	6
Sm	4.6	4.1	5.2	5.9	3	4.8	7	1.9
Eu	0.7	1.2	1.1	1.3	0.3	0.9	1.3	0.7
Gd	3.6	4.1	3.9	5	2.7	4.3	6.2	2
Tb	0.5	0.7	0.6	0.8	0.5	0.7	1	0.4
Dy	2.9	4	3.3	4.7	2.7	4.3	6.7	2.4
Ho	0.4	0.7	0.6	0.9	0.4	0.7	1.3	0.4
Er	1.2	2	1.7	2.6	1	1.9	3.9	0.9
Tm	0.2	0.3	0.3	0.4	0.1	0.3	0.6	0.1
Yb	1.1	1.9	1.7	2.4	0.8	1.7	3.8	0.8
Lu	0.2	0.3	0.3	0.3	0.1	0.3	0.6	0.1
V	11	84	21	67	< 5	< 5	58	< 5
Cr	< 20	30	< 20	30	< 20	< 20	30	< 20
Co	2	10	3	12	1	1	5	1
Ni	< 20	20	< 20	20	< 20	< 20	< 20	< 20
Cu	< 10	< 10	< 10	< 10	< 10	< 10	< 10	< 10
Zn	60	70	40	70	60	40	90	30
Pb	44	31	26	19	58	60	28	69
Ga	18	19	16	17	19	16	21	13
Ge	2	2	1	2	3	2	2	3
Th	13.5	7.7	14.7	12.2	7.9	13.2	12.8	2.3
U	7.7	2.1	2.3	2.1	7.5	3.6	2.5	2.3

Note: Sample: NM - Nam Meng; NR - Nam Rom; SM - Song Ma; KB - Kim Boi; ML - Muong Lat; PSL - Pu Si Lung; SS - Sam Son; Rock type: GBD - gabbro diorite; GND - granodiorite; QD - quartz diorite; BAG - biotite-amphibole granite; BG - biotite granite; BMG - biotite-muscovite granite (two micas granite)

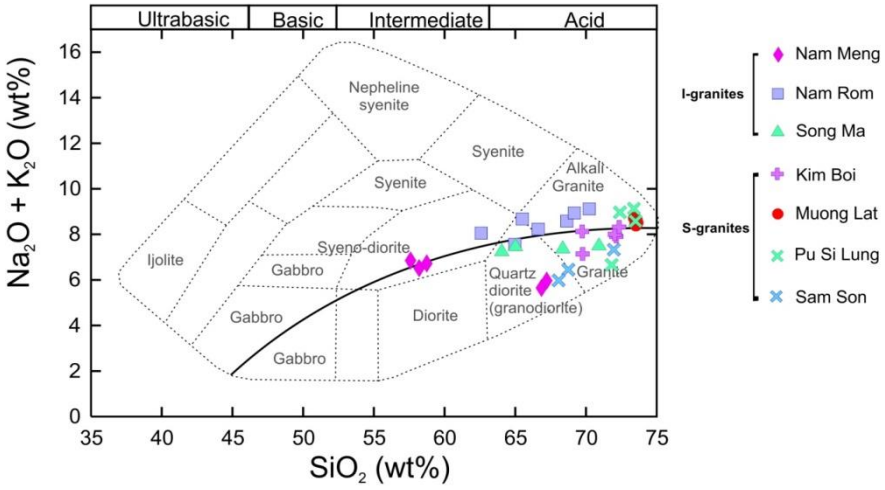

Figure 3. Classification of granite on basis of (SiO_2 - Na_2O+K_2O)

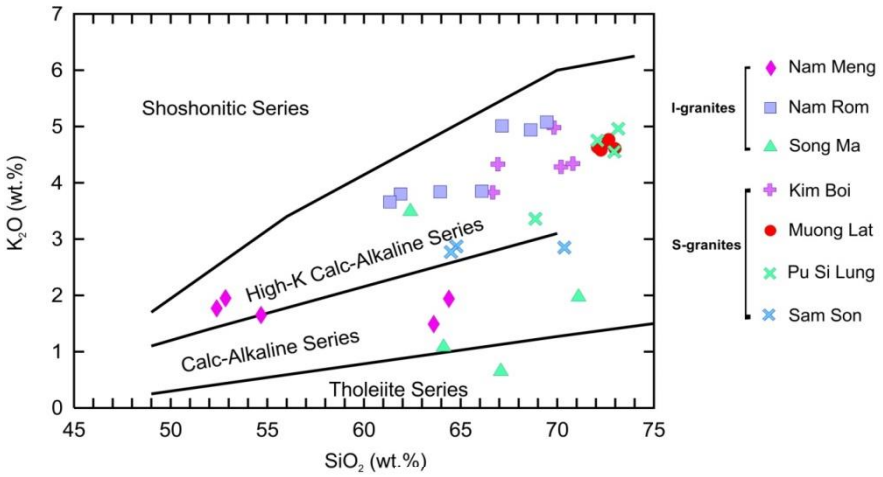

Figure 4. Classification of I-type and S-type granites on basis of SiO_2-K_2O

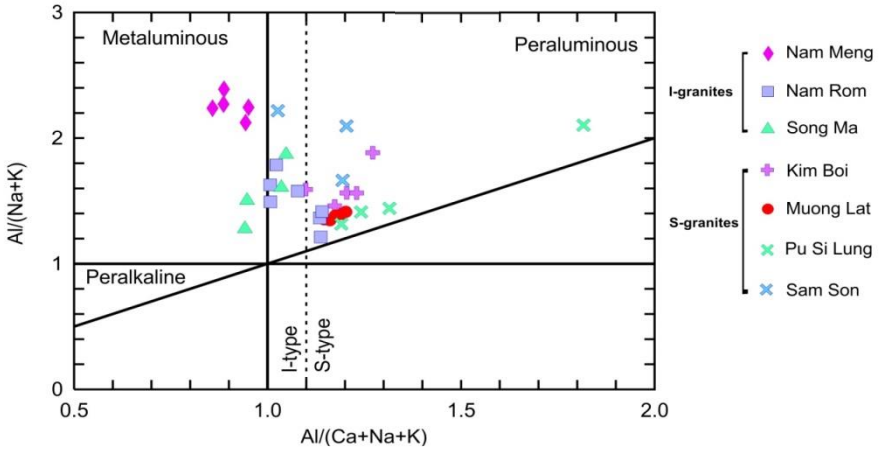

Figure 5. Classification of I-type and S-type granites on basis ASI [Al_2O_3/(Na_2O+K_2O) - Al_2O_3/(CaO+Na_2O+K_2O)

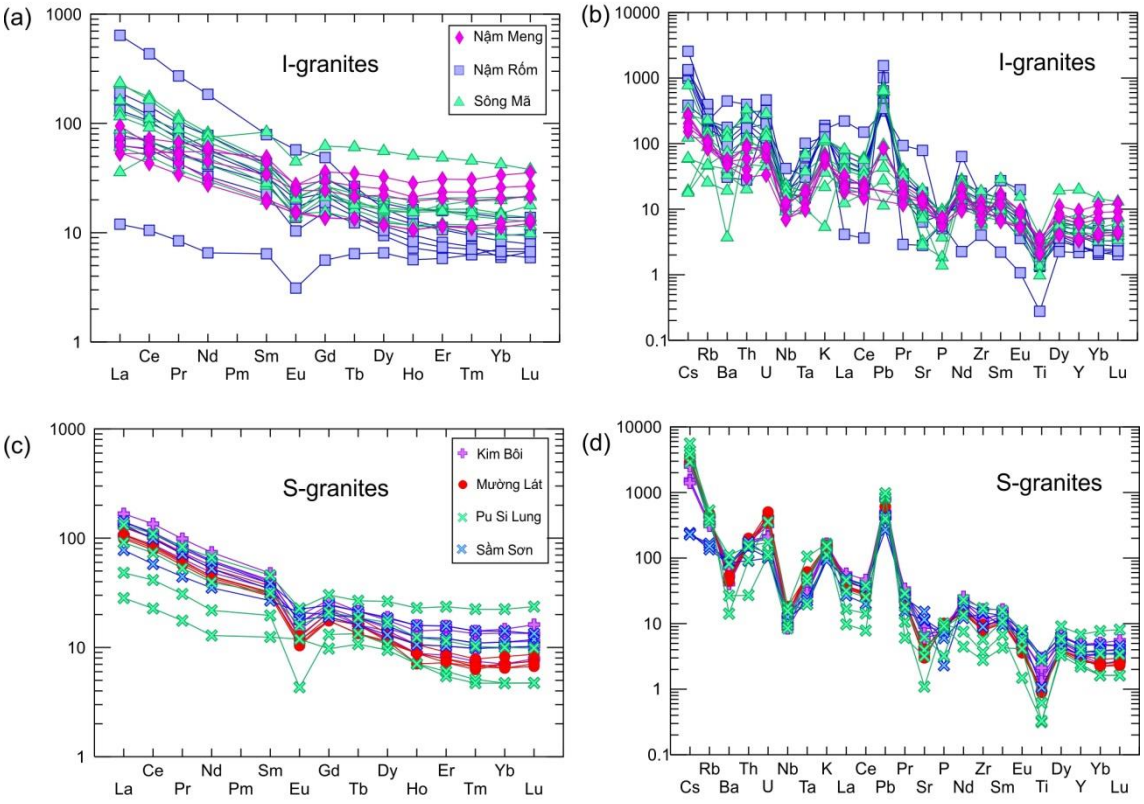

Figure 6. CI chondrite normalized REE patterns (a and c) and primitive mantle (PM) normalized spider diagrams (b and d) of the TSBF I-type (a and b) and S-type (c and d) granites

Nd and Sr isotopic ratios from seven samples of the Nam Rom and Song Ma massifs have been determined (Table 5). The $^{87}Sr/^{86}Sr$ values of the Nam Rom granitoid vary in a wide range from 0.7072 to 0.7319 and low ƐNd(230 Ma) (-12.21 to -6.67). Similar to Nam Rom pluton, the Song Ma granite has low $^{87}Sr/^{86}Sr$(230 Ma) (0.7097 to 0.7186) and low ƐNd(230 Ma) (-10.40 to -7.83). The data of this study overlap with the reported data of Lan et al. (2000) and Liu et al. (2012) for Nam Rom ($^{87}Sr/^{86}Sr(i)$ = 0.7121-0.7370; ƐNd(t) = (-9.7) - (-4.8)), and I-type granite (247Ma) from Sam Nua (Laos) ($^{87}Sr/^{86}Sr(i)$ = 0.7122; ƐNd(t) = -8.7; Tran et al., 2019). The Nd model age (T_{DM}) of the Nam Rom and Song Ma massifs are 1.03-2.38 and 1.01-1.77 billion years, respectively (Table 5).

Table 5. Sr-Nd isotopes of I-type and S-type granites in TSBF (this study)

Sample	NR-9/1	NR-9/3	NR-9/4	NR-9/5	SM-2/2	SM-10/1	SM-10/2	KB18-01	KB18-02
Rock type	BAG	GND	QD	BAG	QD	BAG	GND	BG	BG
$^{87}Rb/^{86}Sr$	5.07	0.24	1.09	2.83	1.07	0.69	0.45	9.05	6.28
$^{87}Sr/^{86}Sr$	0.7395	0.7076	0.7192	0.7329	0.7202	0.7115	0.7104	0.7584	0.7532
$(^{87}Sr/^{86}Sr)_{230\ Ma}$	0.7319	0.7072	0.7175	0.7286	0.7186	0.7105	0.7097	0.7288	0.7326
$^{147}Sm/^{144}Nd$	0.1377	0.0847	0.1209	0.138	0.1118	0.1237	0.1299	0.1448	0.1395
$^{143}Nd/^{144}Nd$	0.512	0.5123	0.512	0.512	0.5121	0.5122	0.5122	0.5119	0.5119
$(^{143}Nd/^{144}Nd)i$	0.5118	0.5121	0.5119	0.5118	0.5119	0.512	0.512	0.5117	0.5117
$eNd_{(t)}$	-12.12	-6.67	-11.17	-12.21	-10.4	-7.83	-8.33	-12.42	-11.7
TDM (Ga)	2.36	2.36	1.83	2.38	1.60	1.59	1.77	2.71	2.47

Table 5 (cont.)

Sample	KB18-07	KB18-11	KB18-15	ML18-01	ML18-07	ML18-08	ML18-09	ML18-14
Rock type	BG	GND	GND	BMG	BMG	BMG	BMG	BMG
$^{87}Rb/^{86}Sr$	3.36	4.24	4.52	9.74	10.17		11.94	13.32
$^{87}Sr/^{86}Sr$	0.7341	0.7366	0.7438	0.7634	0.7561		0.7684	0.777
$(^{87}Sr/^{86}Sr)_{230\ Ma}$	0.7231	0.7227	0.729	0.7315	0.7228		0.7293	0.7335
$^{147}Sm/^{144}Nd$	0.1336	0.1289	0.1302	0.144	0.1424	0.1439	0.1411	0.1406
$^{143}Nd/^{144}Nd$	0.5119	0.5119	0.5119	0.512	0.512	0.512	0.512	0.512
$(^{143}Nd/^{144}Nd)i$	0.5118	0.5118	0.5117	0.5118	0.5118	0.5118	0.5118	0.5118
$eNd_{(t)}$	-11.05	-10.89	-11.77	-10.04	-10.26	-10.58	-9.82	-10.11
TDM (Ga)	2.24	2.11	2.22	2.42	2.4	2.48	2.31	2.33

4.2.2. The S-type granites

The granitoids from Kim Boi, Muong Lat, and Sam Son plutons contain dominantly granite (SiO_2 = 68.87-72.99 wt.%) and minor granodiorite (SiO_2 = 64.50-66.93 wt.%). All rocks have low to intermediate Al_2O_3 (13.61-16.29 wt.%, mostly 14-15 wt.%); the granodiorite is low in alkali (Na_2O+K_2O = 5.20-6.26 wt.%), while the granite is higher (Na_2O+K_2O = 7.05-8.35 wt.%, mostly 7 wt.%) (Table 4; Fig. 3). The Pu Si Lung, Kim Boi, Muong Lat, and Sam Son granitoids are mostly calc-alkaline rocks; some of Kim Boi samples are shoshonite (Fig. 4). The ASI (A/CNK) varies from 1.10-1.85, reflecting a peraluminous S-type granite characteristic (Fig. 5). The S-type granitic rocks are rich in Rb (196-331 ppm) except Pu Si Lung pluton (86-105 ppm); Ba (186-569 ppm); Sr (63-189ppm), Zr (31-184), Nb (6-13 ppm) but lower compared to I-type granites (Table 4; Fig. 6D). The ratios of K/Rb, Rb/Sr, and Rb/Ba varies from 161-188; 0.37-3.50; and 0.15-0.98, respectively. The concentration of Th, U, Ta, Y in S-type are similar to their concentration in I-type granite (Table 4; Figs. 6B, D). The S-type granites are rich in rare earth elements (ΣREE = 38-160 ppm); the ratios of $[La/Sm]_N$, $[La/Yb]_N$ and $[Gd/Yb]_N$ varies from 2.28-3.90, 5.93-16.76, and 1.72-2.93, respectively. The Kim Boi and Muong Lat granitoids have higher concentrations of LREE than those of the Pu Si Lung and Sam Son massifs (Fig. 6C). The S-type granites are low in Ba, Nb, Ta, Ti, Sr, and rich in Rb, Th, U, and have flat HREE patterns (Fig. 6D). Those characteristics are identical for granitic rocks within the TSFB (Tran et al., 2008).

Nd-Sr isotopic ratios of ten samples from Kim Boi and Muong Lat massifs have been determined (Table 5). They have high $^{87}Sr/^{86}Sr$ values (0.7227-0.7335), low of ƐNd(t) (-12.4 to -9.8), which is identical for the S-type granites that originated from the crust. The Nd model ages (T_{DM2}) are 2.11-2.71 billion years (Table 5). The low ƐNd(t) values of the S-type granitic rocks indicate a crustal source, which is similar to the reported ƐHf(t) of Muong Lat (-11.3 to -9.9; Thanh et al., 2019) and Hai Van (-9.2 to -8.4; Hieu et al., 2015), which have the Hf model age a bit younger (T_{DM2} = 1.90-1.99 and 1.66-1.81, respectively).

5. Discussions

5.1. Petrogenesis of the I-type and S-type granites

This study's results and reported data of the whole-rock $^{87}Sr/^{86}Sr(i)$, ƐNd(t), and zircon ƐHf(t) have been listed in Table 6. Previous studies have reported three scenarios of the origin of the I-type granites in the TSFB: (1) lower crust protolith, (2) crustal protolith with minor portion of mantle, (3) mixing of felsic and mafic magmas. The crustal protolith was determined as metagraywacke or metamorphosed magmatic rocks (Qian et al., 2019). Lan et al. (2000) and Liu et al. (2012) suggested that magmas forming TSFB granitoids were originated from partial melting of the crust with a minor portion of the mantle. While Hieu et al. (2017) and

Liu et al. (2012) debated that the Nam Meng granitoid was formed from a mantle-derived magma with a minor portion of crust (ƐHf(289-296Ma) = +5 to +8); and the Nam Rom granite (ƐHf(220-240Ma) = -8.9 to -6; ƐNd(t) = - 8.85 to - 9.58) formed by partial melting the crust with a minor portion of the mantle. The origin of S-type granites has been reported as partial melting of the paleo-crust (Hieu et al., 2017; 2020; Thanh et al., 2019) ($^{87}Sr/^{86}Sr(i)$ = 0.7145-0.7487; ƐNd(t) = -8 to -12; ƐHf(t) = -8 to -11).

Table 6. List of Sr-Nd, Lu-Hf isotopes of I-type and S-type granites in TSBF and Northeast Laos

Rock type	Ages (Ma)	Area	$^{87}Sr/^{86}Sr(i)$	ƐNd(t)	ƐHf(t)	T_{DM2} (Ga)	Source
Subduction-related magmatic assiociations							
Diorite (I-granite)	289-296	Nam He (Nam Meng) Vietnam			(+5.1) - (+7.9)	0.63-0.76	Hieu et al., 2015
Granodiorite (I-granite)	286-290	Pha Lek (Laos)			(+4) - (+10)	0.6-1.3	Hou et al., 2019
Dioritic gabbro	281-276	Muong Lay (Vietnam)	0.705	+0.1		1.76	Liu et al., 2011
Granodiorite, Bt-Amf granite (I-type)	281-276	Muong Khoun (Laos)			(+7.8) - (+13.8)	0.37-0.61	Qian et al., 2019
Bt granite (I-S transition type)	274-258	Xam Nuea, Muong Khoun (Laos)			(-1.1) - (-8.8)	1.36-1.66	Qian et al., 2019
Diorite, granodiorite, Bt-Amf granite (I-granite)	255-270	Xiang Khuang, Muong Khoun (Laos)	0.70548-0.71103	(-2.4) - (-1.5); (-8.8)- (-8.4)	(-3.51) - (+0.37)	1.13-1.71	Hoa et al., 2020
Diorite (I-type)	260-263	Song Ma (Vietnam)			(+7)-(+13.9)	0.34-0.61	Hieu et al., 2017
Rhyolite (I-type)	261	NE Xam Nuea (Laos)			(-4.7)-(-14.7)	1.42-1.97	Qian et al., 2019
Syn-collisional magmatic associations							
Bt-Grn granite (S-type granite)	255-251	Sam Neua, Xiang Khoang, Nam Phao (Laos)	0.71158-0.72524	(-7.1) - (-13.4)	(-7.61) - (-44.82)	1.76-2.56	Hoa et al., 2020
Bt granite (S-type)	244	Dien Bien (Vietnam)			(-10) - (-6)	1.17-1.35	Hieu et al., 2015
Bt and Bt-Ms granite	251-242	Kim Boi, Muong Lat	0.7227-0.7335	(-9.8) - (-12.4)		2.11-2.71	This study
Bi granite (cordierite-containing)	246-242	Hai Van (Vietnam)	0,7145-0,7487	(-8.2) - (-13.3)	(-8) - (-11)		Anh et al., 1995; Hieu et al., 2015
Dacite, rhyolite	252	Xiang Khuang (Laos)	0.7108-0.7146	(-7) - (-10.1)		1.60-1.85	Hoa et al., 2020
Post-collisional magmatic associations							
Bt-Amf granite (I-type)	247-244	Xam Neua (Laos)	0.7101-0.7122	(-8.6) - (-8.7)	(-1.38) - (-8.62)	1.73-1.74	Hoa et al., 2020
Granodiorite, Amf granite	234-221	Sam Nuea, Muong Khoun (Laos)			(+4.2) - (+5)	0.6-0.89	Qian et al., 2019
Diorite, granodiorite, Nam Rom (I-granite)	230	Dien Bien (Vietnam)			(-8.9) - (-6)	1.13-1.23	Hieu et al., 2015
Diorite, granodiorite and granite of Nam Rom and Song Ma intrusions (I-granite)	227-228	Nam Rom, Song Ma (Vietnam)	0.7072-0.7319	(-12.21) - (-6.67)		1.01-2.38	This study
Granodiorite	229	Nam Rom	0.715	-8.9		1.76	Liu et al., 2011

Based on reported whole-rock Nd-Sr, Hf zircon, Usuki and Tran (2020) proposed two events of magma mixing (272-257 Ma and 255-244 Ma) for the I-type and S-type granites TSFB. However, the magma mixing model did not work for the Permian-Triassic I-type and S-type granites of Dien Bien, Song Ma, Muong Lat, and Kim Boi massifs (Fig. 7). Therefore, we conclude that the mantle-derived with a minor portion of the crust is a suitable explanation for the formation of Nam Meng I-type granite (ƐHf(t)= +5 to +7) and other granitoids along the Dien Bien Phu fault. The partial melting lower crust can explain the formation of the Nam Rom and Song Ma diorite-granodiorite-granite series. It is also possible that the mixing of 290-270 Ma dioritic magma with the felsic magma can lead to the formation of the Nam Rom and Song Ma granites, the occurrences of the mafic xenoliths in the rocks could be evidence for the magma mixing.

The occurrences of the sedimentary enclaves, rich alumina minerals (sillimanite, cordierite, muscovite), high $^{87}Sr/^{86}Sr(i)$ (0.7227-0.7335), and low ƐNd(t) (-12.4 to -9.8) with T_{DM2} = 2.11-2.17 Ga, indicate a source of partial melting the Paleoproterozoic crust for the S-type granites of Kim Boi, Muong Lat, and Sam Son massifs. The subduction model was used to explain the partial melting of the crustal material to form the Permian-Triassic granitic rocks of the TSFB (Hieu et al., 2015,

2017, Qian et al., 2019, Wang et al., 2016, Shi et al., 2015, Liu et al., 2012). However, there are ideas of mantle plumes playing an essential role in providing the heat to melt the lithosphere forming the Permian-Triassic granitic rocks of the TSFB (Owada et al., 2016; Faure et al., 2018; Pham-Ngoc et al., 2020).

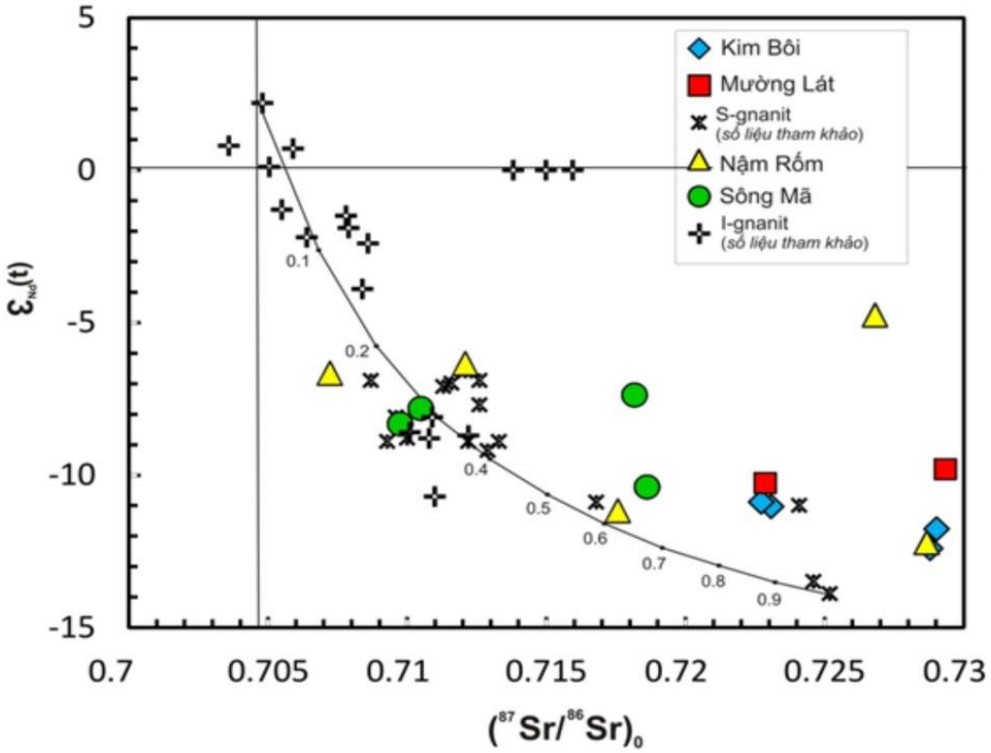

Figure 7. ƐNd(t) vs $^{87}Sr/^{86}Sr(i)$ of the Permian-Triassic granitoids from NW Vietnam (this study) and NE Laos (Usuki and Hoa, 2020)

5.2. U-Pb zircon geochronology

5.2.1. Outline of published data

Several publications have reported the U-Pb ages of I-type and S-type granites of TSFB using the LA-ICP-MS method; their data has been listed in Table 7.

The reported data include: (1) Nam Meng diorite and gabbro diorite have the U-Pb age of 276 Ma (Liu et al., 2012), or 289-296 Ma (Hieu et al., 2017); (2) Nam Rom granodiorite and Bt-Amf granite have younger U-Pb age of 244-233 Ma (Hieu et al., 2019), or 229-217 Ma (Liu et al., 2012); (3) Kim Boi Bt granite has U-Pb age of 242 Ma (Tran et al., 2016); (4) Pu Si Lung Bt granite has U-Pb age of 260 Ma (U-Pb, TIMS; Bui et al., 2010); (5) Muong Lat biotite granite and two micas granite have U-Pb ages of 251-242 Ma. (Thanh et al., 2019). Therefore, the I-type granitoids of the TSFB were formed in two stages at 290-270 Ma (Nam Meng) and 245-220 Ma (Nam Rom). The earlier stage formed the plutons in the western side of the Dien Bien Phu fault, including Nam Meng (and Muong Tung); the later stage formed the plutons in the eastern side of the Dien Bien Phu fault, containing Nam Rom and Song Ma plutons. The formation ages of the Kim Boi and Muong Lat granitoids are 251-242 Ma.

Table 7. U-Pb, Th/U ratios and ages of the Permian-Triassic granitoids Nam Rom and Song Ma intrusions in the NW Vietnam

Spot	Isotopic ratios						Age (Ma)				Dis (%)	Th/U ratio
	$^{207}Pb/^{206}Pb$	±1s	$^{207}Pb/^{235}U$	±1s	$^{206}Pb/^{238}U$	±1s	$^{207}Pb/^{235}U$	±1s	$^{206}Pb/^{238}U$	±1s		
Song Ma Granodiorite												
SM6-4	0.0555	0.0030	0.3036	0.0206	0.0397	0.0009	269	16	251	6	7	0.3610
SM6-8	0.0565	0.0040	0.2878	0.0244	0.0369	0.0009	257	19	234	6	9	0.3636
SM6-2R	0.0543	0.0020	0.2760	0.0144	0.0369	0.0009	247	11	233	5	6	0.3279
SM6-5	0.0552	0.0029	0.2784	0.0185	0.0366	0.0009	249	15	232	5	7	0.4367
SM6-6	0.0566	0.0049	0.2845	0.0291	0.0365	0.0009	254	23	231	6	9	0.7813
SM6-21	0.0585	0.0007	0.2934	0.0076	0.0364	0.0008	261	6	230	5	12	0.4651
SM6-12	0.0540	0.0006	0.2693	0.0072	0.0362	0.0008	242	6	229	5	5	0.3067
SM6-13	0.0542	0.0018	0.2699	0.0131	0.0361	0.0009	243	10	229	5	6	0.3021
SM6-2	0.0521	0.0006	0.2600	0.0063	0.0362	0.0008	235	5	229	5	3	0.3650
SM6-22	0.0521	0.0006	0.2597	0.0070	0.0362	0.0008	234	6	229	5	2	0.4082
SM6-23	0.0545	0.0030	0.2713	0.0191	0.0361	0.0009	244	15	229	5	6	0.3636
SM6-15	0.0512	0.0006	0.2540	0.0063	0.0360	0.0008	230	5	228	5	1	0.2247
SM6-20	0.0528	0.0006	0.2594	0.0070	0.0357	0.0008	234	6	226	5	3	0.4274
SM6-19	0.0545	0.0006	0.2670	0.0069	0.0356	0.0008	240	6	225	5	6	0.4274
SM6-16	0.0530	0.0021	0.2579	0.0138	0.0353	0.0008	233	11	224	5	4	0.3289
SM6-9	0.0521	0.0006	0.2538	0.0065	0.0353	0.0008	230	5	224	5	3	0.3257
SM6-3	0.0532	0.0019	0.2578	0.0130	0.0351	0.0008	233	11	223	5	4	0.2398
SM6-11	0.0523	0.0034	0.2534	0.0200	0.0352	0.0008	229	16	223	5	3	0.4854
SM6-17	0.0518	0.0006	0.2504	0.0066	0.0351	0.0008	227	5	222	5	2	0.3049
SM6-18	0.0529	0.0031	0.2547	0.0184	0.0349	0.0008	230	15	221	5	4	0.4484
SM6-10	0.0552	0.0006	0.2626	0.0069	0.0345	0.0008	237	6	219	5	8	0.3509
SM6-7	0.0576	0.0039	0.2624	0.0214	0.0330	0.0008	237	17	209	5	12	0.2525
Nam Rom Granodiorite												
NR8-22	0.0532	0.0007	0.2845	0.0084	0.0388	0.0009	254	7	245	6	4	0.1733
NR8-19	0.0512	0.0041	0.2691	0.0263	0.0382	0.0010	242	21	241	6	0	0.2062
NR8-20R	0.0516	0.0006	0.2637	0.0071	0.0371	0.0009	238	6	235	5	1	0.2079
NR8-7	0.0517	0.0006	0.2631	0.0069	0.0369	0.0009	237	6	234	5	1	0.2571
NR8-18	0.0482	0.0041	0.2449	0.0247	0.0368	0.0010	222	20	233	6	-5	0.7042
NR8-13	0.0512	0.0006	0.2554	0.0070	0.0362	0.0008	231	6	229	5	1	0.3215
NR8-5	0.0518	0.0006	0.2584	0.0069	0.0362	0.0008	233	6	229	5	2	0.2618
NR8-24	0.0499	0.0006	0.2476	0.0070	0.0360	0.0009	225	6	228	5	-1	0.1980
NR8-12	0.0505	0.0006	0.2505	0.0063	0.0360	0.0008	227	5	228	5	0	0.1953
NR8-15	0.0504	0.0006	0.2498	0.0065	0.0359	0.0008	226	5	228	5	-1	0.2128
NR8-11	0.0519	0.0006	0.2566	0.0068	0.0359	0.0008	232	5	227	5	2	0.1938
NR8-6	0.0514	0.0006	0.2540	0.0066	0.0359	0.0008	230	5	227	5	1	0.2445
NR8-8	0.0501	0.0013	0.2466	0.0105	0.0357	0.0008	224	9	226	5	-1	0.1761
NR8-14	0.0500	0.0006	0.2464	0.0062	0.0358	0.0008	224	5	226	5	-1	0.2188
NR8-16	0.0520	0.0006	0.2546	0.0066	0.0355	0.0008	230	5	225	5	2	0.2618
NR8-4	0.0520	0.0006	0.2525	0.0065	0.0352	0.0008	229	5	223	5	3	0.1938
NR8-17	0.0506	0.0006	0.2470	0.0064	0.0354	0.0008	224	5	224	5	0	0.2188
Nam Rom Gabbro diorite												
NR3	0.0611	0.0007	0.4306	0.0114	0.0511	0.0012	364	8	321	7	12	2.3256
NR3-5	0.0629	0.0007	0.3591	0.0089	0.0414	0.0010	312	7	262	6	16	2.7027
NR3-6	0.0588	0.0128	0.3435	0.0822	0.0424	0.0013	300	62	268	8	11	0.0407
NR3-8	0.0576	0.0006	0.3200	0.0082	0.0403	0.0010	282	6	255	6	10	1.5385
NR3-9	0.0506	0.0006	0.2687	0.0071	0.0385	0.0009	242	6	244	6	-1	0.0285
NR3-11	0.0573	0.0007	0.3038	0.0081	0.0385	0.0009	269	6	243	6	10	2.0000
NR3-14	0.0544	0.0007	0.2842	0.0081	0.0379	0.0009	254	6	240	6	6	0.1316
NR3-2	0.0486	0.0060	0.2535	0.0349	0.0378	0.0009	229	28	239	6	-4	1.4085
NR3-13	0.0547	0.0006	0.2848	0.0074	0.0377	0.0009	254	6	239	6	6	0.2532
Nam Rom Bt-Amf granite Nam Rom												
NR15-2C	0.0541	0.0010	0.3089	0.0118	0.0414	0.0010	273	9	261	6	4	0.1835
NR15-2R2	0.0522	0.0007	0.2604	0.0076	0.0362	0.0009	235	6	229	5	3	0.1748
NR15-4	0.0507	0.0006	0.2501	0.0069	0.0358	0.0009	227	6	227	5	0	0.2427
NR15-2R	0.0501	0.0006	0.2469	0.0071	0.0357	0.0009	224	6	226	5	-1	0.2066
NR15-1	0.0491	0.0006	0.2405	0.0064	0.0355	0.0009	219	5	225	5	-3	0.1678
NR15-3	0.0510	0.0007	0.2453	0.0071	0.0349	0.0008	223	6	221	5	1	0.2817

5.2.2. New results of this study

Four samples from the Nam Rom gabbro-diorite (NR3), Nam Rom granodiorite (NR8), Nam Rom Bt-Amf granite (NR15), and Song Ma granodiorite (SM6) have been dated by U-Pb zircon to clarify the timing of the I-type granitoids.

Fourteen zircon grains have been analyzed from sample NR-3. However, only the U-Pb isotopes of 6 grains yielded relevant results. Most data of NR-3 are discordant, but the best coherent population (Fig. 8A) delivers a weighted-mean 206Pb/238U age of 246 ± 10 Ma (n=6; MSWD = 2.7). Zircons are 40-100µm in length; dark CL images have weak or non-zonation structures and subhedral to anhedral forms. The interior parts of these zircons have Th/U ratios ranging from 0.02-2.70 (Table 7), in which No. 6 and No. 9 spots have Th/U ratios of 0.03 and 0.04, which are characteristic of metamorphic zircon whereas the others are indicative of magmatic of zircon (Hoskin and Schaltegger, 2003).

Twenty-four zircon crystals were analyzed from sample NR-8. Zircons are 70-150µm in length, sharp prismatic, dark CL-images with zonation structure. NR-8 zircons have Th/U ratios ranging from 0.18-0.70 (Table 7), indicating a magmatic origin (Hoskin and Schaltegger, 2003). Data of NR-8 are concordant and form a coherent population (Fig. 8B), yielding a weighted-mean $^{206}Pb/^{238}U$ age of 228±2.6 Ma (n=15; MSWD = 0.47).

Five zircon grains were analyzed from sample NR-15. Zircons are divided into two populations based on length; one group is 60-150µm, whereas the other mostly exceed 250µm. The zircons are subhedral to euhedral; some grains have dark CL-images with a non-zonation structure. NR-15 zircons have Th/U ratios (0.17-0.28, Table 7), indicating of magmatic zircons (Hoskin and Schaltegger, 2003). Data of NR-15 are concordant and form a coherent population (Fig. 7), yielding a weighted-mean $^{206}Pb/^{238}U$ age of 225.6± 4.4 Ma (n = 5; MSWD = 0.35). One zircon crystal has a giant core with the weighted average $^{206}Pb/^{238}U$ of 261.6±6 Ma, different with the rim 226-229±5 Ma and may indicate inheritance of basement rocks.

Twenty zircon crystals were analyzed from sample SM-6. Zircons are 100-150µm in length, prismatic, and have a clear zonation structure. The sector zoned domains of the interior part of these zircons have Th/U ratios ranging from 0.22-0.78 (Table 7), which are considered to be magmatic in origin (Hoskin and Schaltegger, 2003). Most data of SM-6 are concordant and form a coherent population (Fig. 8D), yielding weighted-mean $^{206}Pb/^{238}U$ age of 227.3±2.3 Ma (n=19; MSWD=0.56).

Our data reporting a 245-225 Ma formation age overlaps with the reported data of Liu et al. (2012) and Hieu et al. (2017, 2019). The similar U-Pb age of Song Ma and Nam Rom granites reflects a synchronic formation. In addition, they have similar characteristics of whole-rock geochemistry. Therefore, the Nam Rom and Song Ma granitoids are suggested to categorize into the same complex.

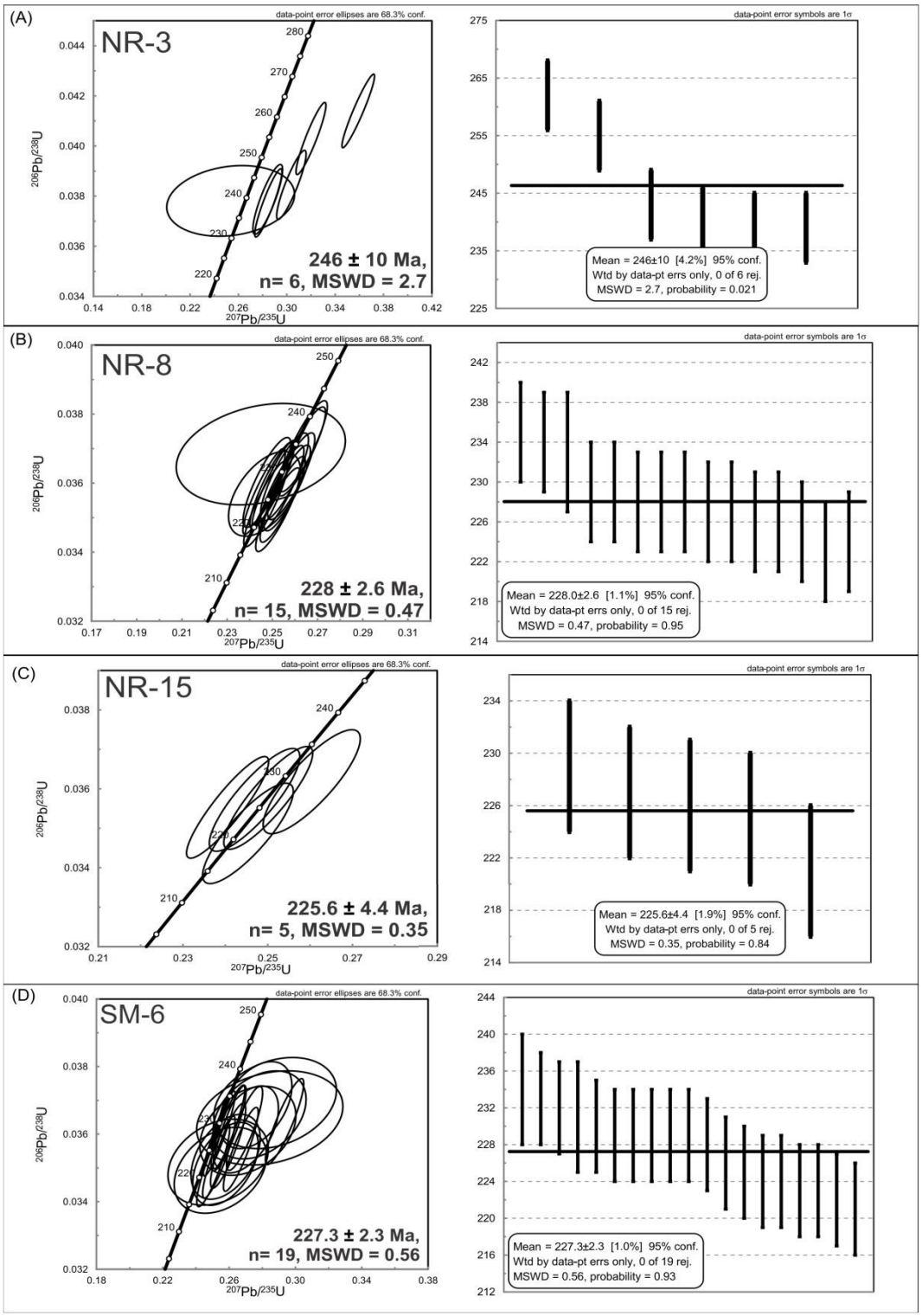

Figure 8. Concordia plots of the in-situ zircon data from the Nam Rom diorite (A - NR-3), Nam Rom granodiorite (B - NR-8), and granite (C - NR-15), and Song Ma granodiorite (D - SM-6)

5.3. Tectonic settings

Discussion on the tectonic setting related to the formation of TSFB granitoids is quite complicated. Considering the I- and S-type granitoids on the tectonic discrimination diagram (Pearce, 1984), most data are plotted in the volcanic arc granites (VAG), except several data of the Pu Si Lung, Kim Boi, Muong Lat, and Sam Son granitoids are syn-collisional granites (syn-COLG) (Figs. 9A, B). Although the Pu Si Lung granite is syn-COLG, Pu Si Lung may not relate to the syn-collision as Kim Boi, Muong Lat, and Sam Son granitoids because of their older formation age (260 Ma; Bui et al., 2010), thus, requires further consideration.

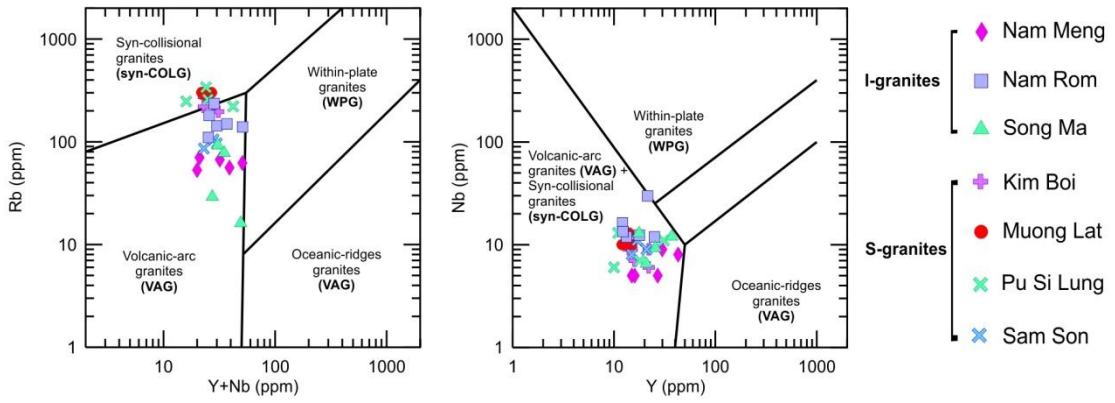

Figure 9. Tectonic discrimination diagram of I-type and S-type granites from the TSFB (Pearce, 1984)

Previous studies on dynamic models have distinguished the amalgamation of the Indochina and the Sino-Vietnam Composite Terranes into three tectonic events: subduction, collision, and post-collision (Tran et al., 2008; 2015; Lan et al., 2000; Liu et al., 2012; Hieu et al., 2015; 2017; Tran et al., 2019; Lai et al., 2014; Shi et al., 2015). The subduction event is considered as the major geodynamic to create the TSFB. The differences of each model include (1) period of subduction, collision, and post-collision, (2) subducted direction, and (3) their geodynamic. Tran et al. (1977) reported that the suture of Indochina and South China Block started during Neoproterozoic and the Indochina Terrane was subducted beneath the Sino-Vietnam Composite Terrane. However, other studies reported that the subduction appeared later in Paleozoic, and the Sino-Vietnam Composite Terrane subducted beneath the Indochina Terrane (Lai et al., 2014; Liu et al., 2012; Lepvrier et al., 2008; Hieu et al., 2015, 2017; Shi et al. 2015; Tran et al., 2008, 2019).

This study proposes a subduction model at 290-270 Ma, collision at 255-245 Ma, and post-collision at 235-225 Ma. The Nam Meng I-type granitoid was generated during the subduction period, the Kim Boi, Muong Lat, and Sam Som S-type granitoids were formed during the collision, and the Nam Rom and Song Ma I-type granitoids were formed during the post-collision period. The Pu Si Lung granitoid needs to be carefully studied before being put into this model.

Most previous studies have considered the closure of Paleo-Tethys and the amalgamation of the Indochina and the Sino-Vietnam Composite Terranes as the major dynamic to create the TSFB granitoids. However, Wang et al. (2016) suggested that the closure of Paleo-Tethys and open of Meso-Tethys played a major role in the convergence of the

Sibumasu, Qamdo-Simao-Indochina, and Sino-Vietnam blocks and indicated the role of Emeishan Plume activity as one dynamic factor. Shellnutt et al. (2020) has proposed the paleo-location of NW Vietnam during 260-257 Ma in the center of Emeishan Large Igneous Province (ELIP). The relation to ELIP activities is a unique characteristic of NW Vietnam and the western side of the Sino-Vietnam terrane during the Permian period. As the TSFB granites lay on the west side of the ELIP during the Permian period, it could be possible that the formation of TSFB rocks has been affected by ELIP.

The appearance of N-MORB and E-MORB mafic magmatism, including metabasalt, metagabbro, and plagiogranite was reported in the Sop Hao area (Houaphanh, Laos; Tran et al., 2019), whereas gabbro and plagiogranite were found in the Tri Nang massif (Thanh Hoa, Vietnam; Hung et al., 2019). The magmas have a composition similar to an ophiolite unit that raises doubt on the current regional tectonic setting models, thus requiring more studies to address the issues.

6. Conclusions

Based on the mineralogical, geochemical, and geochronological characteristics of the Permian-Triassic granitoids in Northwest Vietnam, their relations to the amalgamation of the Indochina and Sino-Vietnam composite terranes have been concluded:

(1) The Nam Meng I-type granitoid was formed during the subduction of Sino-Vietnam Composite Terrane beneath the Indochina Terrane at 290-280 Ma. The magma was mantle-derived with a minor input of crustal material.

(2) The Kim Boi, Muong Lat, and Sam Son S-type granitoids were formed during the syn-collision period at 251-242 Maby matured crust melting.

(3) The Nam Rom and Song Ma I-type granitoids were formed during the post-collision period at 242-225 Ma. The magma source was the lower crust with a minor input of mantle-derived.

Acknowledgments

The Vietnam Academy of Science and Technology (VAST) funded this research project, coded KHCBTĐ.01/18-20. The authors acknowledge the assistance of Drs. Ngo Thi Phuong, Pham Thi Dung, Bui An Nien, Bui Thi Sinh Vuong, and Ms. Ngo Thi Huong during the research progress and manuscript preparation. Dr. Nguyen Hoang is thanked for his comments on an earlier version of the manuscript. CPN and SD are grateful for VAST funding support to QTLA01.02/18-19 (IGS-VAST). TTP would like to acknowledge the funding support from the grant of Taiwan MOST 109-2116-M-002-013- to Prof. Ching-Hua Lo (NTU).

References

Dao D.T., Huynh T., 1995, Geology of Vietnam. Volume II: Magmatic formations, Ha Noi. General Department of Geology and Minerals of Vietnam, 360pp.

Dovjikov A.E., Bui P.M., Vasilevskaja E.D., Zhamoida A.I., Ivanov G.V., Izokh E.P., Le D.H., MaReitchev A.I., Nguyen V.C., Nguyen T.T., Tran D.L., Pham V.Q., Pham D.L., 1965. Geology of North Vietnam - Explanatory note to the Geological map of Northern Vietnam on 1:500.000 scale. Science and Technics Publishing House.

Faure M., Nguyen V.V., Luong T.T.H., Lepvrier C., 2018. Early Paleozoic or Early-Middle Triassic collision between the South China and Indochina Blocks: The controversy resolved? Structural insights from the Kon Tum massif (Central Vietnam). Journal of Asian Earth Sciences, 166, 162-180.

Hieu P.T., Li S.-Q., Yu Y., Thanh N.X., Dung L.T., Tu V.L., Siebel W., Chen F., 2017. Stages of late Paleozoic to early Mesozoic magmatism in the Song

Ma belt, NW Vietnam: evidence from zircon U-Pb geochronology and Hf isotope composition: International Journal of Earth Sciences, 106(3), 855-874.

Hieu P.T., Nong T.Q.A., Pham M., Nguyen T.B.T., 2019. Geochemistry, zircon U-PB ages and HF isotopes of the Muong Luan granitoid pluton, Northwest Vietnam and its petrogenetic significance. Island Arc, 29(1), e12330.

Hieu P.T., Yang Y.Z., Do Q.B., Nguyen B.T., Le T.D., Chen F., 2015. Late Permian to Early Triassic crustal evolution of the Kontum massif, central Vietnam: zircon U-Pb ages and geochemical and Nd-Hf isotopic composition of the Hai Van granitoid complex. International Geology Review, 57, 1877-1888.

Hoskin P.W.O., 2003. The Composition of Zircon and Igneous and Metamorphic Petrogenesis: Reviews in Mineralogy and Geochemistry, 53(1), 27-62.

Hung T.Q., Xuan P.T., Nien B.A., Polyakov G.V., Shelepaev R.A., Tung V.D., Cong T.Q., 2019. Composition characteristics and age of Tri Nang intrusion, Northwest Vietnam, in Proceedings International Symposium on the 35th Anniversary of Collaboration between the Institute of Geological Sciences, VAST and the Institute of Geology and Mineralogy, SB-RAS "Geology and Metallogeny of Vietnam". Publishing House for Science and Technology, Hanoi, 131-138.

Lan C.Y., Chung S.L., Shen J.J.-S., Lo C.H., Wang P.L., Tran T.H., Hoang H.T., Mertzman S.A., 2000. Geochemical and Sr-Nd isotopic characteristics of granitic rocks from northern Vietnam. Journal of Asian Earth Sciences, 18(3), 267-280.

Liu J., Tran M.-D., Tang Y., Nguyen Q.-L., Tran T.-H., Wu W., Chen J., Zhang Z., Zhao Z., 2012. Permo-Triassic granitoids in the northern part of the Truong Son belt, NW Vietnam: Geochronology, geochemistry and tectonic implications. Gondwana Research, 22(2), 628-644.

Metcalfe I., 2013. Gondwana dispersion and Asian accretion: Tectonic and paleogeographic evolution of eastern Tethys. Journal of Asian Earth Sciences, 66, 1-33.

Owada M., Osanai Y., Nakano N., Adachi T., Kitano I., Tri T.V., Kagami H., 2016. Late Permian plume-related magmatism and tectonothermal events in the Kontum Massif, central Vietnam. Journal of Mineralogical and Petrological Sciences, 111(3), 181-195.

Pearce J.A., Harris N.B.W., Tindle A.G., 1984. Trace element discrimination diagrams for the tectonic interpretation of granitic rocks. Journal of Petrology, 25, 956-983.

Pham-Ngoc C., Tran T.A., Tran T.H., Vu H.L., Pham Thi P.L., Ngo T.H., 2020. Chemical compositions of amphiboles and their references to formation conditions of granitoids from Nam Rom and Song Ma massifs, Northwest Vietnam. Vietnam Journal of Earth Sciences, 42, 80-92.

Qian X., Wang Y., Zhang Y., Zhang Y., Senebouttalath V., Zhang A., He H., 2019. Petrogenesis of Permian-Triassic felsic igneous rocks along the Truong Son zone in northern Laos and their Paleotethyan assembly. Lithos, 328-329, 101-114.

Roger F., Jolivet M., Maluski H., Respaut J., Müncha P., Paquette J., Vu Van T., Nguyen V.V., 2014. Emplacement and cooling of the Dien Bien Phu granitic complex: implications for the tectonic evolution of the Dien Bien Phu Fault (Truong Son Belt, NW Vietnam). Gondwana Research, 26, 785-801.

Sakata S., Hattori K., Iwano H., Yokoyama T.D., Danhara T., Hirata T., 2014. Determination of U-Pb ages for young zircons using laser ablation-ICP mass spectrometry coupled with an ion detection attenuator device. Geostandards and Geoanalytical Research, 38, 409-420.

Shellnutt J.G., Pham T.T., Denyszyn S.W., Yeh M.-W., Tran T.A., 2020. Magmatic duration of the Emeishan large igneous province: Insight from northern Vietnam. Geology, 48(5), 457-461.

Shi M.F., Lin F.C., Fan W.Y., Deng Q., Cong F., Tran M.D., Zhu H.P., Wang H., 2015. Zircon U-Pb ages and geochemistry of granitoids in the Truong Son Terrane, Vietnam: Tectonic and Metallogenic implications. Journal of Asian Earth Sciences, 101, 101-120.

Stacey J.S., Kramers J.D., 1975. Approximation of terrestrial lead isotope evolution by a two-stage model: Earth and Planetary Science Letters, 26, 207-221.

Stern R.A., 1997. The GSC sensitive high ion microprobe (SHRIMP): analytical techniques of zircon U-Th-Pb age determinations and performance evaluation: Geological Survey of Canada Current Research, Radiogenic Age and Isotopic Studies. Report, 10, 1-32.

Thanh T.V., Hieu P.T., Minh P., Nhuan D.V., Thuy N.T.B., 2019. Late Permian-Triassic granitic rocks of Vietnam: the Muong Lat example. International Geology Review, 61, 1823-1841.

Tran T.H., Izokh A.E., Polyakov G.V., Borisenko A.S., Ngo T.P., Balykin P.A., Tran T.A., Rudnev S.N., Vu V.V., Bui A.N., 2008. Permo-Triassic magmatism and metallogeny of North Vietnam in relation to Emeishan's Plume. Russian Geology and Geophysics, 49, 480-491.

Tran T.H., Lan C.-Y., Usuki T., Shellnutt J.G., Pham T.D., Tran T.A., Pham-Ngoc C., Ngo T.P., Izokh A.E., Borisenko A.S., 2015. Petrogenesis of Late Permian silicic rocks of Tu Le basin and Phan Si Pan uplift (NW Vietnam) and their association with the Emeishan large igneous province. Journal of Asian Earth Sciences, 109, 1-19.

Tran T.H., Polyakov G.V., Tran T.A., Borisenko A.S., Izokh A.E., Balykin P.A., Ngo T.P., Pham T.D., 2016. Intraplate Magmatism and Metallogeny of North Vietnam, Switzerland. Springer International Publishing, XII, 372pp.

Tran T.H., Tran T.A., Ngo T.P., Pham T.D., Tran V.A., Izokh A.E., Borisenko A.S., Lan C.Y., Chung S.L., Lo C.H., 2008. Permo-Triassic intermediate-felsic magmatism of the Truong Son belt, eastern margin of Indochina: Comptes Rendus Geoscience, 340(2-3), 112-126.

Tran T.H., Tran T.A., Pham-Ngoc C., Izokh A.E., Goryachev N.A., Usuki T., Pham T.D., Lien P.T.P., Bui A.N., 2019. Permian - Triassic magmatism related to amalgamation Indochina - Sino-Vietnam composite terranes, in Proceedings Conference on the Basic studies in "Earth Sciences and Ecology" - CARRES, Ho Chi Minh City. Publishing House for Science and Technology, 37-41.

Tran V.T., Vu K., 2011. Geology and Earth Resources of Vietnam, Ha Noi. Publishing House for Science and Technology, 646pp.

Tran V.T., Faure M., Nguyen V.V., Bui H.H., Fyhn M.B.W., Nguyen T.Q., Lepvrier C., Thomsen T.B., Tani K., Charusiri P., 2020. Neoproterozoic to Early Triassic tectono-stratigraphic evolution of Indochina and adjacent areas: A review with new data: Journal of Asian Earth Sciences, 191, 104231.

Tran V.T., Nguyen V.C., Le V.C., Duong X.H., Le H., Vu K., Pham D.L., Pham K.N., Tran D.N., Hoang H.Q., Tong D.T., Phan T.T., Trinh T., Nguyen T., Nguyen X.T., Nguyen D.U., 1977. Geology of Vietnam - the North part. Explanatory note to the geological map on 1:1.000.000 scale. Science and Technics Publishing House, 354pp.

Usuki T., Tran T.H., 2020. Petrogenesis of Permo-Triassic post-collisional magmatism in the Truong Son belt, northern Laos, in Proceedings AGU Fall Meeting.

Usuki T., Lan C.-Y., Tran T.H., Pham T.D., Wang K.-L., Shellnutt G.J., Chung S.-L., 2015. Zircon U-Pb ages and Hf isotopic compositions of alkaline silicic magmatic rocks in the Phan Si Pan-Tu Le region, northern Vietnam: Identification of a displaced western extension of the Emeishan Large Igneous Province. Journal of Asian Earth Sciences, 97, 102-124.

Wang S., Mo Y., Wang C., Ye P., 2016. Paleotethyan evolution of the Indochina Block as deduced from granites in northern Laos: Gondwana Research, 38, 183-196.

Woods G., 2017. Lead isotope analysis: removal of ^{204}Hg isobaric interference on ^{204}Pb using ICP-QQQ MS/MS reaction cell, Handbook of ICP-QQQ Applications using the Agilent 8800 and 8900, 141p.

Zaw K., Meffre S., Lai C.-K., Burrett C., Santosh M., Graham I., Manaka T., Salam A., Kamvong T., Paul C., 2014. Tectonics and metallogeny of mainland Southeast Asia - A review and contribution. Gondwana Research, 26(1), 5-30.

Zhao S.W., Lai S.C., Pei X.Z., Qin J.F., Zhu R.Z., Tao N., Gao L., 2019. Compositional variations of granitic rocks in continental margin arc: Constraints from the petrogenesis of Eocene granitic rocks in the Tengchong Block, SW China. Lithos, 326-327, 125-143.